A telomerase with novel non-canonical roles: TERT controls cellular aggregation and tissue size in *Dictyostelium*

Short title: Telomerase TERT controls tissue size in *Dictyostelium*

Nasna Nassir[1], Geoffrey J. Hyde[2], Ramamurthy Baskar[1]

[1]Department of Biotechnology, Bhupat and Jyoti Mehta School of Biosciences, Indian Institute of Technology-Madras, Chennai, India

[2] Independent Researcher, 14 Randwick St, Randwick, New South Wales, Australia.

* Corresponding author

E-mail: rbaskar@iitm.ac.in (RB)

Abstract

Telomerase, particularly its main subunit, the reverse transcriptase, TERT, prevents DNA erosion during eukaryotic chromosomal replication, but also has poorly understood non-canonical functions. Here, in the model social amoeba *Dictyostelium discoideum*, we show that the protein encoded by *tert* has telomerase-like motifs and regulates, non-canonically, important developmental processes. Expression levels of wild-type (WT) *tert* were biphasic, peaking at 8 and 12 h post-starvation, aligning with developmental events, such as the initiation of streaming (~7 h) and mound formation (~10 h). In *tert* KO mutants, however, aggregation was delayed until 16 h. Large, irregular streams formed, then broke up, leading to small mounds. The mound-size defect was not induced when a KO mutant of *countin* (a master size-regulating gene) was treated with TERT inhibitors but anti-countin antibodies did rescue size in the *tert* KO. Further, conditioned medium from *countin* mutants failed to rescue size in the *tert* KO, but the converse experiment worked. These and additional

observations indicate that TERT acts upstream of *smlA/countin* to regulate tissue size: (i) the observed expression levels of *smlA* and *countin*, being respectively lower and higher (than WT) in the *tert* KO; (ii) the levels of known size-regulation intermediates, glucose (low) and adenosine (high), in the *tert* mutant, and the size defect's rescue by supplementing glucose or the adenosine-inhibitor, caffeine; (iii) the induction of the size defect in the WT by *tert* KO conditioned medium and TERT inhibitors. The *tert* KO's other defects (delayed aggregation, irregular streaming) were associated with changes to cAMP-regulated processes (e.g. chemotaxis, cAMP pulsing) and their regulatory factors (e.g. cAMP; *acaA*, *carA* expression). Overexpression of WT *tert* in the *tert* KO rescued these defects (and size), and restored a single cAMP signalling centre. Our results indicate that TERT acts in novel, non-canonical and upstream ways, regulating key developmental events in *Dictyostelium*.

Author summary

When cells divide, their chromosomes are prone to shrinkage. This risk is reduced by an enzyme that repairs protective caps on each chromosome after cell division. This enzyme, telomerase, also has several other important but unrelated roles in human health. Most importantly, via one or other of its functions, both high and low levels of the enzyme can contribute to cancer. We have studied, for the first time, the roles played by telomerase in the life-cycle of the cellular slime mould, *Dictyostelium discoideum*, a model system with a rich history of helping us understand human biology. While we did not find any evidence of telomerase having the features typically needed to repair a chromosome, telomerase was necessary for many aspects of development. In forming the fruiting bodies that help *Dictyostelium* reproduce, a mutant that lacks telomerase miscalculates how big those bodies should be, and they end up being too small. Also, earlier, during an earlier stage, aggregation,

the migration of cells that form each fruiting body is delayed and irregular. These results are significant because they show, for the first time, that a telomerase can influence cell migration and tissue size regulation, two processes involved in a wide range of cancers.

Introduction

Each time a chromosome replicates, it loses some DNA from each of its ends. This is not necessarily problematic, because the chromosome is initially capped at each end by a sacrificial strand of non-coding DNA, a telomere [1-3]. Further instances of replication, however, can expose the coding DNA, unless the cell can keep repairing the shortened telomeres, by the action of the enzyme complex, telomerase. Accordingly, telomerase, whose main subunits comprise a reverse transcriptase (TERT), and the telomerase RNA component (TERC) [4], has much significance in the biology and pathology of multicellular organisms. As somatic tissues age, for example, telomerase is downregulated, and the resulting telomeric dysfunction can lead to chromosomal instability and various pathologies, including disrupted pregnancies and cancer [5-7]. In other cases, the upregulation of telomerase is also associated with, and a biomarker of, some cancers, because it allows the unchecked proliferation of immortalised tumour cells [6, 8]. Telomerase also has many non-canonical roles, in which telomere maintenance, or even telomerase activity, is not required [9, 10]. For example, telomerase is known to have non-canonical roles in neuronal differentiation [11], RNA silencing [12], enhanced mitochondrial function [13] and various cancers [9, 14].

Our understanding of telomeres and telomerase began, and has continued to develop, through the study of model organisms such as *Drosophila*, *Zea mays*, *Tetrahymena*, yeast and mice [2, 3, 15-19]. One model system in which the possible roles of telomerase have not yet been

addressed is *Dictyostelium discoideum*. This system has proved its usefulness in many contexts, including the study of human diseases [20-24]. One of its advantages is that the processes of cell division (i.e. growth) and development are uncoupled [25], making the organism a highly tractable system for the study, in particular, of differentiation and tissue size regulation [26-33]. In culture, when its bacterial food source is abundant, *D. discoideum* multiplies as single-celled amoebae. This leads to denser colonies, and exhaustion of the food supply. The rising concentration of a secreted glycoprotein, CMF, triggers the organism to switch to a multicellular mode of development [32, 34]. With no resources for further cell proliferation, the amoebae move, in a radial pattern of streams, towards centres of aggregation. Rising levels of secreted proteins, of the counting factor (CF) complex [35, 36], trigger a series of changes that lead to breaking up of the streams, which therefore no longer contribute cells to the original aggregate. Each aggregate, which will typically contain 20, 000 to 100,000 cells [37], now rounds up into a mound, which then proceeds through several life-cycle stages, finally forming a spore-dispersing fruiting body about 1-2mm high [32, 38]. Mounds can also develop from the breaking-up of a large stream (or aggregate), a process similarly regulated by CF [27, 39]. The generic term, ‘group’, can be used to address the fact that mounds develop from clusters that arise in these slightly different ways, but in this paper we will refer to ‘mounds’. Some of the processes and regulators involved in our very abbreviated account of the life-cycle are shown in Fig 1, which focuses on those elements examined in this study.

In addition to being uncoupled from growth, development in *D. discoideum* has other features that make it potentially useful as a model system for the understanding of telomerase-based pathologies, in particular cancers that arise from disruption of non-canonical functions. First, as indicated in Fig 1, development in *D. discoideum* depends on properly regulated cell motility and cell adhesion, two processes fundamental to metastasis. Second, the switch to

multicellular development, and the control of aggregate, mound and hence fruiting body size are influenced by various secreted factors that, respectively, promote aggregation and regulate tissue size, in ways analogous to the regulation of tumour size by chalones [40, 41]. Third, a putative TERT has been annotated in the *D. discoideum* genome. It is not known if the RNA component of telomerase (TERC) is present [42] and, in any case, extrachromosomal rDNA elements at the ends of each chromosome in *D. discoideum* suggest a novel telomere structure [43]. Thus, telomerase in this organism may have a separate mechanism for telomere addition or might have non-canonical roles. As yet, however, there have been no functional studies of TERT reported for *D. discoideum*.

In this study, we characterize the gene *tert* in *D. discoideum*, showing that it has both RT and RNA binding domains. We describe the pattern of *tert*'s expression levels during all stages of development, assay for any canonical telomerase function, and examine the effects of knocking out the gene's function on development. The *tert* mutant exhibits a wide range of developmental defects, suggesting that wild-type TERT targets multiple elements of the regulatory network depicted in Fig 1. Most interestingly, these defects, and the results of experiments by which we attempt to rescue, or phenocopy, the *tert* KO phenotype, suggest that this telomerase influences the activity of *smlA*, and processes downstream of it. *Tert* thus emerges as the most upstream gene involved in the cell-counting pathway identified to date, and its overall influence indicates that, despite having no obvious canonical activity, a telomerase can nevertheless play major regulatory roles by virtue of its non-canonical targets.

Results and discussion

D. discoideum expresses *tert*, a gene encoding a protein with telomerase motifs

Extending previous predictions of *tert* encoding a protein with telomerase motifs [44], our use of the Simple Modular Architecture Research Tool (http://SMART.embl-heidelberg.de) and UniProt (Q54B44) revealed the presence of a highly conserved reverse transcriptase domain and a telomerase RNA binding domain (S1 Fig). These are characteristic of a telomerase reverse transcriptase [45], supporting the idea that the gene we characterize below indeed encodes for TERT. The protein shares 23% and 18.7% identity with human and yeast TERT protein respectively (Pairwise sequence Alignment-Emboss Needle).

Telomerase activity, if any, is ascertained by performing a Telomeric Repeat Amplification Protocol (TRAP) assay. However, while human cell lines (HeLa, HEK) showed telomerase activity, we did not detect any telomerase activity in *D. discoideum* cell extracts (S2 Fig). This concurs with previous findings, namely that the telomeres of *D. discoideum* have a novel structure [46], and that, in other organisms, TERT has several non-canonical roles [11-13].

Constitutive expression of telomerase during growth and development in *D. discoideum*

In humans, telomerase expression is reported to be low in somatic cells compared to germline and tumour cells [47]. To ascertain if *tert* expression is differentially regulated during growth and/or development, we performed qRT-PCR using RNA from different developmental stages (0, 4, 8, 10, 12, 16 and 24 h after starvation). *Tert* expression is higher in development than during growth, (8h and 12 h) (Fig 2), implying that *tert* plays a prominent role beyond the point at which *D. discoideum* is responding to starvation. Expression also shows a marked biphasic pattern, with the first peak at 8h (when streams are forming), a big dip during stream breaking (10h) and then rising gradually again to peak at about the time of mound formation (16h).

143

144 ***tert* KO leads to delayed development, irregular streaming, and smaller mounds and**
145 **fruiting bodies**

146 To understand the possible non-canonical roles of *tert* in development in *D. discoideum*, *tert*
147 KO cells generated by homologous recombination were seeded at a density of $5x10^5$
148 cells/cm^2 on non-nutrient buffered agar plates and monitored throughout development. While
149 aggregates appeared by 8 h in the wild-type, and streams began to break at 10 h, in the
150 mutants there was a further 8 h delay before aggregates were seen, and stream breaking
151 began at about 18 h. Wild-type cells formed long streams of polarized, elongated cells
152 leading to aggregation but *tert* KO cells did not form well-defined streams, failing to
153 aggregate even at $5x10^4$ cells/cm^2 (wild-type cells aggregated at a density of $2x10^4$ cells/cm^2),
154 suggesting an inability to respond to aggregation-triggering conditions (S3 Fig). The mutant's
155 streams were also larger (Fig 3A). In contrast to streams moving continuously towards the
156 aggregation centre in WT, *tert* KO streams break while they aggregate (Supplementary
157 Videos 1 and 2). They did eventually form aggregates, largely by clumping. During the early
158 stages of aggregate formation, the number of aggregates formed by the *tert* KO was only
159 10% of that formed by WT (Fig 3B, $p<0.0001$). Due to uneven fragmentation, the late
160 aggregates were also of mixed sizes. The *tert* KO cells did eventually form all of the typical
161 developmental structures, but by the mound stage, continued fragmentation had resulted in
162 the mounds being more numerous, and smaller, on average, than in the WT. This was also the
163 case for fruiting bodies. Thus, with reference to Fig 1, *tert* appears to play roles in multiple
164 aspects of *Dictyostelium* development: the timing of aggregation; streaming, and the
165 regulation of the size of the mound and fruiting body (Table 1).

Table 1a. Phenotypic differences between wild-type and *tert* KO development of *D. discoideum*, and some possible causal factors (Part 1 of 2)

	Timing of delay to aggregation	Streaming and Aggregation	Mound (and fruiting body) size	Mound-size regulation pathway		
				***smlA* expression levels**	***Countin* expression levels**	**Glucose levels**
Wild-type cells	Normal	Normal	Normal	Normal	Normal	Normal
tert KO cells	Delayed (by 8h)	Fragmented, uneven aggregates	Small	Low	High*	Low*

Green shading indicates normal (wild-type) levels, or activity. Red shading indicates abnormally high or low levels. *Asterisks refer to atypical processes (or levels) in the *tert* KO cells for which rescue attempts were made (see Table 2).

Table 1b. Phenotypic differences between wild-type and *tert* KO development of *D. discoideum*, and some possible causal factors (Part 2 of 2)

	cAMP-related factors (streaming & delay regulation)					Adhesion-related factors (in streaming and mound-size regulation)			Delay-specfiic regulation
	Levels of cAMP-related genes: acaA, carA, 5'NT, pdsA, regA, pde4	**Adenosine/ 5'NT Levels**	**cAMP *centres***	**cAMP levels**	***cAMP-based chemotaxis***	***csaA, cadA* expression levels**	**Cell-cell adhesion**	**Cell-substratum adhesion**	**Poly-phosphate levels**
Wild-type cells	Normal	Normal	One	Normal	Normal	Normal	Normal	Normal	Normal
tert KO cells	Low at 4h-10h; High by 12h	High/high during stream break; low after. *	Many*	Low*	Abnormal	Low	Low	Low	Low

Green shading indicates normal (wild-type) levels, or activity. Red shading indicates abnormally high or low levels. *Asterisks refer to atypical processes (or levels) in the *tert* KO cells for which rescue attempts were made (see Table 2).

Many processes and regulators are potentially involved in the phenotypic changes of the *tert* KO

Given the wide-ranging phenotypic defects seen in the *tert* KO, it seemed likely that *tert* is a master regulator, affecting many of the processes and regulators depicted in Fig 1. We thus

monitored the activity or levels of a number of those elements, comparing the wild-type and *tert* KO (summarised in Table 1). As that summary shows, the *tert* KO showed significant changes from the wild-type in three broad areas: components of the mound-size regulation pathway; cAMP-related processes/regulators; adhesion-related processes/regulators. As is clear from Fig 1, the factors that influence these features overlap considerably, both in terms of interacting with each other, and in regulating more than one of the various developmental stages disrupted in the *tert* KO. Nevertheless, we think it is useful to consider each of them in turn. As we do so below, we describe a series of experiments that largely fall into two broad categories, as shown in summary form in Tables 2 and 3: Those that attempt to rescue the normal phenotype in *tert* KO cells (Table 2); and those that attempt to phenocopy, or induce, the *tert* KO phenotype in wild-type cells (Table 3). First, however, we describe some experiments that support the direct involvement of *tert* in the effects already noted.

Table 2. Attempts to rescue normal phenotype (or aggravate[#] the KO phenotype) in *D. discoideum tert* KO cells

	Timing of delay to aggregation	Streaming and Aggregation	Mound and fruiting body size
Overexpression of WT *tert*	Rescue	Rescue	Rescue
Overexpression of human *tert*	No Rescue	No Rescue	No Rescue
WT cells (10-50% of total cells)	Full rescue at 50%	No Rescue	No Rescue
WT Conditioned Medium	No Rescue	No Rescue	No Rescue
Anti-countin or anti-CF50 antibodies	No Rescue	Part Rescue	Part Rescue
Anti-CF45 antibodies	No Rescue	No Rescue	No Rescue
Countin KO Conditioned Medium	No Rescue	No Rescue	No Rescue
1mM glucose	No Rescue	Rescue	Rescue
Caffeine	No Rescue	Rescue	Rescue
cAMP pulsing	No Rescue	No Rescue	No Rescue
8-Br-cAMP	No Rescue	No Rescue	No Rescue
Anti-AprA, anti-CfaD antibodies	No Rescue	No Rescue	No Rescue

tert KO Conditioned Medium [#]	No aggravation (i.e. 8h delay typical of *tert* KO)	Aggravation	Aggravation

Green shading indicates full or partial rescue of normal (wild-type) levels or activity by a treatment applied to *tert* KO cells. Red shading indicates no rescue. The final row refers to an attempt to exacerbate the KO phenocopy.

Table 3. Attempts to phenocopy the *tert* KO phenotype in wild-type *Dictyostelium* cells

	Timing of delay to aggregation	**Streaming and Aggregation**	**Mound and fruiting body size**
tert KO Conditioned Medium	Phenocopies *tert* KO (but delay is only 2h)	Phenocopies *tert* KO	Phenocopies *tert* KO
tert KO cells (90-50%)	Normal	Phenocopies *tert* KO	Phenocopies *tert* KO
200uM iron	Normal	Phenocopies *tert* KO	Phenocopies *tert* KO
BIBR 1532	Normal	Phenocopies *tert* KO	Phenocopies *tert* KO
MST 312	Normal	Phenocopies *tert* KO	Phenocopies *tert* KO
tert KO Conditioned Medium added to WT cells of other Dictyostelids	Normal	Normal	Normal

Red shading indicates full or partial phenocopying of the *tert* KO phenotype by a treatment applied to wild-type cells. Green shading indicates that no phenocopying occurred.

Support for the involvement of *tert* itself in the *tert* KO

To support the idea that the changes observed in the *tert* KO are, in the first instance, due to changes involving *tert* itself, and not some other factor, we took two approaches: Overexpression of *tert*, and the use of TERT inhibitors. Most importantly, overexpression of wild-type TERT (act15/gfp::*tert*) in *tert* KO cells rescued all three of the phenotypic defects (Fig 4A, Supplementary Video 3; Table 2), suggesting that the *tert* KO phenotype is not due to any other mutation. Next, we treated wild-type cells with structurally unrelated TERT specific inhibitors, BIBR 1532 (100nM) and MST 312 (250nM). BIBR 1532 is a mixed-type

non-competitive inhibitor, whereas MST 312 is a reversible inhibitor of telomerase activity (see Methods). Both inhibitors strikingly phenocopied two features of the *tert* mutant, in that we observed large early aggregate streams that broke and eventually resulted in mounds (Fig 4B; Table 3) and fruiting bodies that were small. The developmental delay, however, was not induced. Human TERT [48], which shares a 23% homology with *Dictyostelium* TERT, failed to rescue *tert* KO phenotype. Surprisingly, the morphologies of TERT overexpressing lines in the wild-type did not show any significant variation compared to those of the untreated wild-type (Fig 4A).

Overall, these results strongly support the idea that the relevant change in the *tert* KO involve *tert* itself. The fact that the TERT inhibitors induced only two of the three *tert* KO defects is interesting. Given the lack of any apparent interconnection between the pathway that regulates the switch to aggregation, and that regulating mound size, it seems likely that TERT acts on more than one molecular target. It could be that the inhibitors do not perturb that part of TERT that interacts with the target that regulates the switch to development.

Roles of components of the mound size regulation pathway in the *tert* KO: *smlA*, *CF*, *countin* and glucose

smlA and countin

Compared to the wild-type, in the *tert* KO cells, *smlA* and *countin* expression levels were, respectively, low and high (Figs 5A and 5B; Table 1). Also, Western blots performed with anti-countin antibodies showed higher *countin* expression in *tert* KO cells, compared to wild-type (Fig 5C). When *tert* was overexpressed in the *tert* KO background, both *countin* and *smlA* expression levels were returned to those of the wild-type (Figs 5A and 5B). This overexpression also rescued all the defects of the *tert* KO phenotype (Fig 4A; Table 2). Given

235 the previously proposed regulatory relationship between *smlA* and *countin* (Fig 1; [26, 28,
236 30]), the most parsimonious explanation for the majority of the results reported so far in this
237 study, is that one role of *tert* in *D. discoideum* is to promote the expression of *smlA*, thus
238 indirectly inhibiting *countin* expression, thus reducing glucose levels and mound/fruiting
239 body size. This would make *tert* the most upstream regulator of these structures reported to
240 date.

241 The likelihood of some involvement of CF itself was supported by the effects of antibodies
242 that target its components. When *tert* KO cells were treated with anti-countin or anti-CF50
243 antibodies (1:300 dilution), there was a reduction in aggregate fragmentation resulting in
244 larger mounds compared to untreated *tert* KO controls (Fig 5D; Table 2); the development
245 delay was not rescued. Adding anti-CF45 antibodies did not rescue any of the defects (Fig
246 5D; Table 2).

247 Indirect evidence that *tert* is acting upstream of CF was seen in the lack of effect of adding
248 BIBR 1532 to *countin* KO cells, which typically exhibit no stream breaking and large
249 mounds [28]. While, as noted above, BIBR 1532 leads to stream breaking and small mounds
250 in wild-type cells, it did not lead to any change in the usual phenotype of *countin* KO cells
251 (e.g. Fig 6A), which argues against *tert* acting downstream of *countin*.

252 Beyond the observations already noted, a range of other observations support the idea that
253 some of the *tert* KO's features are due to the increased activity of a secreted mound-size
254 regulating factor, such as countin. Conditioned medium (CM) from *tert* KO cells induced
255 stream breaking in the wild-type (Fig 6B; Table 3) and led to reduced mound size. Also,
256 adding *tert* KO CM to the *tert* KO itself aggravated the fragmentation phenotype (Fig 6B;
257 Table 2). *Tert* KO CM was even capable of inducing stream fragmentation (Fig 6A), and
258 reducing mound size, in *countin* mutants, suggesting that the CF levels of the *tert* KO CM

were high. In each of these three cases, the *tert* KO CM not only affected streaming and mound size, but also induced, or aggravated, a development delay (Figs 6A and 6B; Tables 2 and 3). This suggests that the unknown TERT-induced factor that affects the developmental switch is also secreted.

Further, the presence of *tert* KO cells, even at very low concentrations (10%), was able to partially induce the *tert* KO phenotype when added to a population of wild-type cells and plated at an overall density of $5x10^5$ cells/cm^2 (Fig 6C; Table 3). The apparent potency of the presumed high CF levels produced by the *tert* KO cells might partly explain one otherwise unexpected observation: Adding wild-type CM to *tert* KO cells did not rescue any of their defects (Fig 6B; Table 2). While the wild-type CM in this case would be expected to act as a diluent of CF (and thus potentially rescue the *tert* KO), this effect would only be brief. Development occurs over many hours, during which time the *tert* KO conditions could allow the build-up of CF back to mound-size-limiting levels. Similar reasoning might also explain why CM from *countin* KO cells *(*which exhibit undelayed aggregation and normal streaming) did not rescue any of the defects of *tert* KO cells (Fig 6A; Table 2).

We also observed if *tert* KO CM affected the wild-type cells of other Dictyostelids, such as *D. minutum, D. purpureum, D. fasciculatum* and *Polysphondylium pallidum* (each representing a distinct group in the Dictyostelid taxonomy). CM of *tert* KO did not affect the mound size of any of the species tested (Fig 7; Table 3) suggesting that some of the factors regulating mound size may be species specific.

Glucose rescued streaming and mound size defects, but not the delay

As per the model shown in Fig 1, one of the more downstream effects that should be seen if the *tert* KO has higher levels of CF, is the lowering of glucose levels. Glucose levels during

aggregation were measured and in the *tert* KO were significantly lower (10.7±0.6 mg/ml) compared to wild-type (15.5±0.94 mg/ml) (Fig 8A, p=0.0015). Supplementing 1mM glucose rescued the aggregate streaming (and mound size), defects of the *tert* KO (Fig 8B), but not, as expected, the delay (Table 2).

Antibodies against AprA and CfaD did not rescue the tert KO phenotype

Previous work has shown that deletion of AprA and CfaD genes, involved in a different cell-density sensing pathway to that involving *smlA* and countin, leads to changes in mound-size [29], but, here, antibodies against AprA and CfaD did not rescue the KO phenotype (Fig 9), suggesting, again, that impaired mound size determination in the *tert* KO is largely due to defective CF signal transduction.

Roles of cAMP and cAMP-related processes and factors in the *tert* KO

Given the perturbations seen in the *tert* KO, one would predict some abnormalities associated with cAMP dynamics [49-54]. The role of cAMP in streaming, in particular, has been much studied. Below we examine how various cAMP processes or factors, related to streaming and developmental delay, were affected in the *tert* KO.

Multiple cAMP wave generating centres observed in the tert KO

Starving cells normally aggregate by periodic synthesis and relay of cAMP, resulting in the outward propagation of cAMP waves from the aggregation centres [55]. We visualized cAMP waves by recording the time-lapse of development and then subtracting the image pairs [56]. Coordinated changes in cell shape and movement of cAMP waves can indirectly

306 be visualized by dark field optics because of the differences in the optical density of cells
307 moving/not moving in response to cAMP. Compared to the wild-type, which had a single
308 wave generating centre, the *tert* KO had multiple wave propagating centres (Fig 10,
309 Supplementary Videos 4 and 5). When the *tert* KO was rescued by overexpression of wild-
310 type *tert*, so was the single wave propagating centre. The optical wave density analysis
311 suggests that cAMP wave propagation is defective in *tert* KO, also contributing to stream
312 breaking.

313

314 ***cAMP-related gene expression, cAMP levels, chemotaxis and relay were also impaired in***
315 ***the tert KO***

316 Both the switch to aggregation, and normal streaming, require that a great variety of other
317 cAMP-related processes occur properly. We quantified the relative expression of genes
318 involved in cAMP synthesis and signaling in wild-type and *tert* KO cells by qRT-PCR during
319 streaming as well as breaking (Figs 12A and 12B). With respect to the switch to aggregation,
320 the expression levels of *acaA* (cAMP synthesis), *carA* (cAMP receptor), *5'NT* (5'
321 nucleotidase), *pdsA* (cAMP phosphodiesterases), *regA* and *pde4* were low initially but most
322 started to 'recover' closer to the time that the *tert* KO manages to overcome its
323 developmental delay (Figs 11A-F). Another, perhaps more meaningful, approach is to
324 compare the levels in the mutant and wild-type when they are at equivalent developmental
325 stages. This was done at two stages (aggregation, stream breaking) for four of the cAMP
326 genes (*acaA, carA, pdsA, pde4*). During aggregation (i.e. at 8 h in the wild-type; 16 h in the
327 *tert* KO), *acaA* and *carA* expression levels were significantly lower in the mutant, and the
328 other two genes trended lower (Fig 12A). During stream breaking (10 h; 18 h, respectively),
329 only *acaA* was significantly lower.

Correspondingly, at 8 h of development, cAMP levels were also lower in the *tert* KO (0.98±0.08 nM in the KO; 1.59±0.15 nM in wild-type; Fig 12C, p=0.005). By 12 h, however, as the *tert* KO cells are closer to the time when their streaming will begin (i.e. 16 h) both cAMP-related gene expression, and cAMP levels increase, implying that the initially down-regulated expression of cAMP signaling might explain the long-delayed switch to aggregation in the *tert* KO. As to how cAMP-related genes or processes do recover in the absence of TERT, there are no indications in our results, but regulatory networks are well-known to exhibit a degree of robustness [57, 58].

As noted, cAMP-related gene expression levels of the *tert* KO lag behind that of the wild-type, and even though they increase as the mutant enters a similar developmental phase, the cAMP levels never catch up completely. When cAMP levels were quantified during aggregation and stream breaking using an ELISA-based competitive immunoassay, the cAMP levels in the wild-type and *tert* KO were 1.59±0.15 nM and 1.48±0.25 nM, respectively, during aggregation (Fig 12D, p=0.73); and 1.05±0.11 nM and 0.74±0.70 nM during stream breaking (Fig 12E, p=0.04). Thus, these lower absolute levels of cAMP in the *tert* KO may also contribute to abnormal stream breaking, with the amoebae unable to relay signals to their neighbours.

To test whether cAMP-based chemotaxis was normal, we performed an under-agarose chemotaxis assay, towards 10 µM cAMP. The trajectories of cells were tracked and their chemotaxis parameters were quantified. Although the speed of cells towards cAMP was higher in *tert* KO (16.01±1.39 µm/min) compared to the wild-type (12.74±0.43 µm/min), the directionality was significantly reduced in *tert* KO cells (0.37±0.03 compared 0.59±0.04). The chemotactic index of *tert* KO cells also was lower (0.63±0.05) compared to wild-type cells (0.82±0.06) (Figs 13A-C).

354

355 ***The chemotaxis defect of the tert KO was not rescued by cAMP pulsing or 8-Br-cAMP***

356 To gain further insights into the streaming defect of the *tert* KO cells, we examined if cAMP
357 pulsing could rescue the chemotaxis defect [59, 60]. cAMP (50nM) pulsing was carried out
358 every 6 minutes for 4 hours and thereafter, the cells were seeded in the starvation buffer at a
359 density of $5x10^5$ cells/cm^2 and different developmental stages were monitored (Fig 14A). The
360 streaming defect of *tert* KO was not rescued by cAMP pulsing, suggesting that other
361 components of cAMP signaling are necessary to rescue the defect.

362 If cAMP receptor activity is compromised, that could also lead to defective signaling and to
363 test this, we used a membrane-permeable cAMP analog 8-Br-cAMP, which has poor affinity
364 for extracellular cAMP receptors and enters the cells directly [61]. Cells were incubated with
365 5mM 8-Br-cAMP and after 5 h, the cells were transferred to Bonners Salt Solution and
366 different developmental stages were monitored (Fig 14B). Adding 8-Br-cAMP did not rescue
367 the *tert* KO phenotype, suggesting that cAMP receptor function is not impaired in the mutant.

368

369 ***High adenosine levels in the tert KO induced large aggregation streams***

370 As mentioned previously, adenosine and caffeine are known to alter the cAMP relay [62, 63],
371 thereby affecting aggregate size. This occurs in a number of Dictyostelids [33]. We observed
372 enhanced expression of *5'NT* in the *tert* KO (Fig 15A, p=0.0042) suggesting increased
373 adenosine levels (5'NT converts AMP to adenosine). Hence, adenosine levels were
374 quantified and these were significantly higher (235.37±26.44 nM/10^6 cells) in *tert* KO cells
375 compared to wild-type (35.39±12.78 nM/10^6 cells) (Fig 15B, p=0.0051). The adenosine
376 antagonist, caffeine (1 mM), rescued the streaming defect (Fig 15C), and restored the mound
377 size, suggesting that excess adenosine in the *tert* KO causes larger streams. It did not,

however, rescue the developmental delay. Since glucose also rescues the streaming defect in *tert* KO cells, adenosine levels were quantified subsequent to treating with 1mM glucose. Glucose treatment reduced adenosine levels (13.07±7.51 nM/10^6 cells) in *tert* KO cells to a level that is more comparable to wild-type cells (35.39±12.78 nM/10^6 cells), but as already noted, it did not rescue the developmental delay. Importantly, *5'NT* expression and adenosine levels reduced significantly subsequent to stream breaking (S4 Fig). This could perhaps be due to negative feedback on *tert* itself. When wild-type cells were treated with 2mM adenosine, *tert* expression levels were reduced, although not significantly so (S5 Fig).

Streaming defects of the tert KO were not due to increased iron levels

Dictyostelium cells, when grown in the presence of 200μM iron, formed large streams that fragmented into multiple mounds, strikingly resembling the *tert* KO phenotype [64]. As the phenotypes had similarities, we examined if TERT mediates its effect by altering intracellular iron levels. We quantified iron by ICP-MS and the levels were not significantly different between the wild-type (16.38±1.21 ng/10^7 cells) and *tert* KO cells (15.25±0.81 ng/10^7 cells) (S6 Fig, p=0.4573), suggesting that *tert* KO phenotype is not due to altered iron levels.

The role of adhesion-related factors in the *tert* KO, as they affect streaming and mound size

Cell-substratum adhesion is also important for migration and proper streaming. By spinning cells at different speeds (0, 25, 50 and 75 rpm), it is possible to vary substratum dependent sheer force. Thus, by counting the fraction of floating cells at different speeds, it is possible to check substratum dependent adhesion. Although both wild-type and *tert* KO cells exhibited a sheer force-dependent decrease in cell-substratum adhesion, *tert* KO cells

exhibited a significantly weaker cell-substratum adhesion (Fig 16, $p<0.0001$), thus indicating a contribution to stream breaking.

Cell-cell adhesion is also an important determinant of streaming and mound size in *Dictyostelium* [39]. To examine if adhesion is impaired in the mutant, we checked the expression of two major cell adhesion proteins, *cadA*, expressed post-starvation (2 h) and *csaA* expressed during early aggregation (6 h). *cadA*-mediated cell-cell adhesion is Ca^{2+}-dependent and thus EDTA-sensitive, while *csaA* is Ca^{2+} independent and EDTA-resistant [65]. Both *csaA* and *cadA* expression were significantly down-regulated (Figs 17A and 17B).

Further, cell adhesion was monitored indirectly by counting the fraction of single cells not joining the aggregate. Aggregation results in the gradual disappearance of single cells and thus it is possible to measure aggregation by determining the ratio of single cells remaining. To examine Ca^{2+}-dependent cell-cell adhesion, the assay was performed in the presence of 10 mM EDTA. Both EDTA-sensitive and resistant cell-cell adhesion were significantly defective in *tert* KO cells (Figs 17C, $p=0.0033$ and 17D, $p=0.0015$).

These results imply that defective cell-substratum, and cell-cell adhesion might play roles in the abnormal streaming and mound-size regulation of the *tert* KO.

The developmental delay of the *tert* KO was associated with reduced polyphosphate levels

One interesting observation was that the only treatment that fully rescued the *tert* KO cells was the overexpression of wild-type *tert*. Also, the only other treatment that rescued the developmental delay itself was mixing wild-type cells with the *tert* KO cells at a 1:1 ratio (Fig 18; Table 2). Even though caffeine and glucose rescued streaming and mound size, and apparently this was at least partly mediated via their impact on cAMP-regulated processes,

neither of the compounds rescued the delay, even though abnormalities of cAMP-regulated processes are commonly reported causes of delay in other *Dictyostelium* studies [52-54].

Thus, we examined polyphosphate levels in the *tert* KO because of their known importance to developmental timing in *Dictyostelium* [66]. We stained the CM with DAPI for 5 mins and checked the polyphosphate specific fluorescence using a spectrofluorometer. The CM of *tert* KO cells has reduced polyphosphate levels (49.55±2.02 μM) compared to wild-type (60.62±1.95 μM), implying that low polyphosphate levels might also contribute to the delay in initiating development in this system (Fig 19, p=0.0009).

Conclusions

Our results reveal that TERT plays an important role in many aspects of *Dictyostelium* development. The *tert* KO exhibited a wide range of developmental defects. Despite suitable environmental conditions for multicellular development to begin, the start of the streaming phase is delayed by 8 h. Having once begun, development proceeds and ends abnormally, with large streams, uneven fragmentation, and, eventually, small mounds and fruiting bodies. The wide-ranging developmental defects are associated with changes to the levels, or expression, of genes and compounds that are known to be highly upstream regulators of the various stages of development, such as streaming and mound/fruiting body formation. Based on the perturbations in the *tert* KO, and our other experiments, Fig 20 depicts the possible extent of processes, and potential mediating factors, that might depend upon normal *tert* expression/TERT activity in the wild-type. Note that the arrows that connect *tert*/TERT to any element in the diagram are not meant to suggest that TERT directly regulates that element, only that TERT is important, perhaps in some indirect way, for the normal levels, or activity, of that element.

One of the most striking findings was that TERT appears to regulate, or is at least necessary for, the normal activity of what was previously known as the most upstream regulator of mound size, *smlA* [26, 28, 30]. Expression levels of *smlA* were reduced in the *tert* KO, and we also observed a wide variety of the expected downstream effects of lowered *smlA* levels. All of these, and a wide variety of treatments that rescued the size-defect of the mutant phenotype, support the idea that the reduction of mound size in the *tert* KO was indeed mediated via the abnormal functioning of the previously-identified elements of the mound-size regulation pathway.

In addition to the rescue approach, treatments that attempted to phenocopy the *tert* KO phenotype in the wild-type, also suggest TERT is a highly upstream regulator of mound size. In particular, given that size regulation in *D. discoideum* depends upon secreted factors of the CF complex, one would have predicted the effects we observed when *tert* KO CM was added to wild-type cells. Another strong indication that *tert* acts upstream, at least of CF, was that the inhibition of *tert* activity in *countin* mutants failed to phenocopy the *tert* KO phenotype.

A similarly rich range of results (involving the *tert* KO phenotype, and its rescue, and phenocopying) support the idea that TERT also plays a high-level role in the regulation of streaming. During the streaming phase, two genes associated with cAMP related-processes in *D. discoideum* (*acaA, carA*) were significantly downregulated (compared to the wild-type), and the levels of several other genes trended lower. This was also accompanied by lower cAMP levels. This could explain the defective chemotaxis and cell motility of the *tert* KO.

Of course, the regulation of streaming is not entirely isolated from that of size. Glucose, one of the central elements of the CF pathway, influences several cAMP-related processes [67]. Thus, it was not surprising that adding 1mM glucose to the *tert* KO cells rescued both the size and streaming defects. This study, however, provided a new insight into how the rescue

474 of streaming occurs, because added glucose also reduced adenosine levels. Thus, in the *tert*
475 KO, the low glucose levels might lead to higher adenosine levels, allowing it to inhibit cAMP
476 related processes (via pathway i, Fig 20). In normal development, given that the known
477 sequence of the telomere repeats of *D. discoideum* (A-$G_{(1-8)}$; [43]), and the fact that
478 telomerase activity would therefore recruit cellular stores of adenosine, it is possible that
479 normal TERT activity keeps adenosine levels low. As yet, however, whether TERT actually
480 acts as a functional telomerase in *D. discoideum* is not known.

481 The *tert* gene we characterized includes the conserved domains and structure of a telomerase
482 reverse transcriptase. Also, supplementing structurally unrelated but specific inhibitors of
483 TERT to wild type cells phenocopies the mutant phenotype. The widely used method to test
484 telomerase activity is the TRAP assay. However, this method failed to detect telomerase
485 activity in *D. discoideum* and there may be both technical and innate limitations. For
486 example, possible reasons are that: (i) the presence of rDNA palindrome elements in the
487 chromosomal ends, suggesting a novel telomere structure and the possible role of TERT in
488 maintaining both rDNA and chromosomal termini; and (ii) polyasparagine repeats, present in
489 the TERT protein of *Dictyostelium,* splitting the functional domain into two halves. It is not
490 clear whether the loss of TERT function is due to the absence of normal eukaryote telomeres
491 in *D. discoideum* [68].

492 The discussion so far, while it establishes that TERT is needed for several developmental
493 processes to take place, does not help to distinguish whether or not it acts more than once, or
494 if it has more than one target. Could TERT for example act more like the much studied
495 homeodomain proteins, master regulators of animal development, but which only act during
496 very early embryological life [69, 70]? Likewise, in *D. discoideum,* CMF appears to act only
497 once [32]. Two lines of argument suggest that TERT is different.

First, the biphasic nature of *tert*'s expression pattern suggest that it acts during at least two stages of development. In the wild-type, *tert* expression builds up to its first peak at 8 h, thus being a strong candidate for enabling streaming to begin, and to proceed correctly, around this time. It then dips markedly to a low point at 10 h, whereby it might help to enable stream break-up by its relative absence. Then, it begins its climb to its second peak at 12 h, when mound size is being finalised.

Second, while it is well known that cAMP-related processes play important roles in allowing streaming to begin and to proceed properly, and while we have shown that TERT influences multiple cAMP related processes, the pathway by which TERT influences the initiation of streaming seems distinct from that used for maintaining it. Both glucose and caffeine, for example, rescued the streaming and size defects of the *tert* KO, but the delay was unaffected. Complementarily, when wild-type cells were mixed at 50% with *tert* KO cells, they rescued the delay defect only. In fact, the only treatment that fully rescued the *tert* KO was the overexpression of wild-type *tert*.

This study indicates for, the first time, that TERT acts in several non-canonical ways in *D. discoideum*, influencing when aggregation begins, the processes involved in streaming, and the eventual size of the fruiting body. TERT's influences appear to occur upstream of many other regulators, and, in particular, TERT could be the most upstream regulator of mound and fruiting body size identified so far. Curiously, as yet we have no evidence that TERT acts as a canonical telomerase, nor is it known whether any other enzyme protects the unusually sequenced telomeres of this species. In the most heavily studied stages of the organism's life-cycle, that is, those that occur in response to starvation, replication has ceased, so further study of this particular point should focus on the amoeboid stage. More generally, this study has revealed several previously unreported non-canonical processes influenced by a

522 telomerase. TERT's roles in influencing cell motility and adhesion, and the levels of chalone-
523 like secreted factors, bear consideration by those engaged in cancer research.

524

525 # Methods

526 ## *Dictyostelium* culture and development

527 Wild-type *D. discoideum* (AX2) cells were grown with *Klebsiella aerogenes* on SM/5 plates,
528 or axenically, in modified maltose-HL5 medium (28.4 g bacteriological peptone, 15 g yeast
529 extract, 18 g maltose monohydrate, 0.641 g Na_2HPO_4 and 0.49 g KH_2PO_4 per litre, pH 6.4)
530 containing 100 units penicillin and 100 mg/ml streptomycin-sulphate. Cells were also grown
531 in Petri dishes as monolayers. Other Dictyostelid species (*D. minutum, D. purpureum, D.*
532 *facsiculatum* and *Polysphondylym pallidum*) were grown with *Klebsiella aerogenes* on SM/5
533 plates and cells were harvested when there was visible clearing of bacterial lawns.

534 To trigger development, cells were washed with KK_2 buffer (2.25 g KH_2PO_4 and 0.67 g
535 K_2HPO_4 per liter, pH 6.4) and plated on 1% non-nutrient KK_2 agar plates at a density of
536 $5x10^5$ cells/cm^2 in a dark, moist chamber [71]. To study streaming, cells were seeded in
537 submerged condition (KK_2 buffer) at a density of $5x10^5$ cells/cm^2.

538 BIBR 1532 is a specific non-competitive inhibitor of TERT with IC50 value of 93 nM for
539 human telomerase [72]. To find the optimal dose response of BIBR 1532 in Dictyostelium,
540 starved cells were plated in phosphate buffered agar with different concentrations of BIBR
541 1532 (10 nM, 25 nM, 50 nM, 100nM and 200 nM) and 100nM was found to be the minimal
542 effective dose in inducing complete stream breaking. MST 312, which is structurally
543 unrelated to BIBR 1532, is a reversible inhibitor of TERT with IC50 value of 0.67 µM for

544 human telomerase [73]. The minimal effective dose in *Dictyostelium* was found to be 250
545 nM.

546

547 **Construction of *tert* expression vector**

548 Using genomic DNA as template, a 3.8kb *tert* sequence was PCR amplified using ExTaq
549 polymerase (Takara) and ligated in pDXA-GFP2 vector by exploiting the HindIII and KpnI
550 restriction sites. This vector was electroporated to *tert* KO and AX2 cells and G418 resistant
551 (10 µg/ml) clones were selected and overexpression was confirmed by semi-quantitative
552 PCR. Primer sequences used for generating the vectors are mentioned in S1 Table.

553

554 **Conditioned medium assay**

555 Conditioned medium was prepared as described previously with slight modifications [74].
556 Briefly, log phase cells of AX2 and *tert* KO were resuspended at a density of $1x10^7$ cells/ml
557 and kept under shaking conditions for 20 h. Cells were pelleted and the supernatant was
558 further clarified by centrifugation. The clarified supernatant (CM) was used immediately. To
559 check the effect of CM on aggregate size, cells were developed in the presence of CM on
560 non-nutrient agar plates and development was monitored. KK_2 buffer was used as control. To
561 deplete extracellular CF with anti-countin antibodies, cells were starved in KK_2 buffer. After
562 1 h, the cells were developed with anti-countin antisera (1:300 dilution) in KK_2 [75].

563

564 **Western blot**

565 To examine countin protein expression levels during aggregation, Western blot was
566 performed with anti-countin antibody. Cells were resuspended in SDS laemmli buffer, and

boiled for 3 min. Subsequently, the samples were run in a 12% SDS-polyacrylamide gel and Western blots were developed using an ECL Western blotting kit (Biorad). Rabbit anti-countin antibodies were used at 1: 3000 dilutions.

Cell-cell adhesion assay

Log phase cells were starved at a density of $1x10^7$ cells/ml in KK_2 buffer in shaking conditions at 22 °C for 4 h. At the beginning of starvation, $4x10^7$ cells were removed and resuspended in 2 mL Sorensen phosphate buffer, vortexed vigorously and 0.4 mL of cell suspension was pipetted immediately in vials containing 0.4 ml ice-cold Sorensen phosphate buffer or 0.4 mL of 20 mM EDTA solution. The cell suspension was then transferred to a shaker and incubated for 30 min and 0.2 mL of 10% glutaraldehyde was added to each sample at the end of incubation and stored for 10 min. Then, 7 ml Sorensen phosphate buffer was added to each vial. Cell adhesion was indirectly measured by counting the number of single cells left behind using a hemocytometer [76].

Cell-substratum adhesion

To measure cell-substratum adhesion, $5x10^5$ cells were seeded in 60mm Petri dishes and incubated at 22 °C for 12 hours. The Petri dishes with the cell suspension was placed on an orbital shaker at different speeds (0, 25, 50, 75 rpm). After 1 h, adherent and non-adherent cells were harvested, counted using a hemocytometer and the fraction of adherent cells was plotted against the rotation speed [77].

Visualization of cAMP waves

To visualize cAMP wave propagation, $5x10^5$ cells/cm^2 were plated on 1% non-nutrient agar plates and developed in dark moist conditions at 22 °C. On a real-time basis, the aggregates were filmed at an interval of 30 s/frame, using a Nikon CCD camera and documented with NIS-Elements D software (Nikon, Japan). For visualizing cAMP optical density waves, image pairs were subtracted [56] using Image J (NIH, Bethesda, MD).

Under agarose cAMP chemotaxis assay

The under agarose cAMP chemotaxis assay was performed as described previously [78]. Briefly, 100 µl of cell suspension starved at a density of $1x10^7$ cells/ml in KK_2 buffer was added to outer troughs and 10 µM cAMP was added in the middle trough of a 1% agarose plate. Cells migrating towards cAMP was recorded every 30 s for 15 min with an inverted Nikon Eclipse TE2000 microscope using NIS-Elements D software (Nikon, Japan). For calculating the average velocity, directionality and chemotactic index, each time 36 cells were analyzed. The cells were tracked using ImageJ. Velocity was calculated by dividing the total displacement of cells with time. Directionality was calculated as the ratio of absolute distance traveled to the total path length, where a maximum value of 1 represents a straight path without deviations. Chemotactic index was calculated as the ratio of the average velocity of a cell moving against a cAMP gradient to the average cell speed. It is a global measure of direction of cell motion.

Quantitative real-time PCR (qRT-PCR)

Total RNA was isolated from AX2 and *tert* KO cells at the indicated time points (0–24 h) using TRIzol reagent (Life Technologies, USA) [79]. RNA samples were quantified with a spectrophotometer (Eppendorf) and were also analyzed on 1% TAE agarose gels. cDNA was

614 synthesized from total RNA using cDNA synthesis kit (Verso, Thermo-scientific). 1 µg of
615 total RNA was used as a template to synthesize cDNA using random primers provided by the
616 manufacturer. 1 µl of cDNA was used for qRT-PCR, using SYBR Green Master Mix
617 (Thermo-scientific). qRT-PCR was carried out to analyze the expression levels of *tert*, *acaA*,
618 *carA*, *pdsA*, *regA*, *pde4*, 5'NT, *countin* and *smlA* using the QuantStudio Flex 7 (Thermo-
619 Fischer). *rnlA* was used as mRNA amplification control. All the qRT-PCR data were
620 analyzed as described [80]. The primer sequences are mentioned in S2 Table.

621

622 **cAMP quantification**

623 cAMP levels were quantitated using cAMP-XP TM assay kit as per the manufacturer's
624 protocol (Cell signalling, USA). AX2 and *tert* KO cells developed on 1% KK_2 agar, were
625 lysed with 100 µl of 1X lysis buffer and incubated on ice for 10 min. 50 µl of the lysate and
626 50 µl HRP-linked cAMP solution were added to the assay plates, incubated at room
627 temperature (RT) on a horizontal orbital shaker. The wells were emptied after 3 hours,
628 washed thrice with 200 µl of 1X wash buffer. 100 µl of tetramethylbenzidine (TMB)
629 substrate was added and incubated at RT for 10 min. The reaction was terminated by adding
630 100 µl of stop solution and the absorbance was measured at an optical density of 450 nm. The
631 cAMP standard curve was used to calculate absolute cAMP levels.

632

633 **Glucose quantification**

634 Glucose levels were quantified as per the manufacturer's protocol (GAHK20; Sigma-
635 Aldrich). Mid-log phase cells were harvested and resuspended at a density of $8x10^6$ cells/ml
636 in KK_2 buffer and kept in shaking conditions at 22 °C. Cells were collected again and lysed
637 by freeze-thaw method. 35 µl of the supernatant was mixed with 200 µl of glucose assay

reagent and incubated for 15 minutes. The absorbance was measured at an optical density of 540 nm. The glucose standard curve was used to calculate absolute glucose levels.

Adenosine quantification

Adenosine quantification was performed as per the manufacturer's protocol (MET5090; Cellbio Labs). Cells grown in HL5 media was washed and seeded at a density of $5x10^5$ cells/cm^2 on KK_2 agar plates. The aggregates were harvested using the lysis buffer (62.5mM Tris-HCl, pH 6.8, 2% SDS, 10% glycerol). 50 µl sample was mixed with control mix (without adenosine deaminase) or reaction mix (with adenosine deaminase) in separate wells and incubated for 15 minutes. The fluorescence was measured using a spectrofluorometer (Ex- 550nm, Em- 595nm). The adenosine fluorescence in the sample was calculated by subtracting fluorescence of control mixed sample from reaction mixed sample. The adenosine standard curve was used to calculate absolute adenosine levels.

Polyphosphate measurements

The conditioned media was incubated with 25 µg/ml DAPI for 5 minutes and polyphosphate specific fluorescence was measured using a spectrofluorometer (Ex- 415nm, Em- 550nm) as previously described [81]. Conditioned medium samples were prepared in FM minimal media to reduce the amount of background fluorescence. Polyphosphate concentration, in terms of phosphate monomers were determined using polyphosphate standards.

Microscopy

A Nikon SMZ-1000 stereo zoom microscope with epifluorescence optics, Nikon 80i Eclipse upright microscope or a Nikon Eclipse TE2000 inverted microscope equipped with a digital sight DS-5MC camera (Nikon) were used for microscopy. Images were processed with NIS-Elements D (Nikon) or Image J.

Statistical tools

Microsoft Excel (2016) was used for data analyses. Unpaired student's t-test and two-way ANOVA (GraphPad Prism, version 6) were used to determine the statistical significance.

Acknowledgments

We thank the Dictyostelium Stock Center, USA for supplying *Dictyostelium* strains and plasmids. We thank Dr Richard Gomer (Texas A&M University) for providing countin, CF50, CF45, AprA and CfaD antibodies. Polyphosphate standards were a kind gift from Dr Toshikazu Shiba (RegeneTiss Inc.). hTERT cDNA was a kind gift from Dr. Jayakrishnan Nandakumar (University of Michigan). The telomerase activity assay protocol was suggested by Dr Elizabeth Blackburn. NN acknowledges Rakesh Mani, Shalini Umachandran, Prajna A Rai and J Meenakshi for discussions.

Author Contributions

NN, RB designed the experiments. NN performed the experiments. NN, GH and RB analyzed the data. NN, GH and RB wrote the manuscript and all authors read and approved the final manuscript.

682

683 ## References

684 1. Blackburn EH. Telomeres and telomerase: their mechanisms of action and the effects
685 of altering their functions. Febs Letters. 2005;579(4):859-62. doi:
686 10.1016/j.febslet.2004.11.036.
687 2. Blackburn EH, Gall JG. A tandemly repeated sequence at the termini of the
688 extrachromosomal ribosomal RNA genes in Tetrahymena. Journal of Molecular Biology.
689 1978;120(1):33-53. doi: 10.1016/0022-2836(78)90294-2.
690 3. Greider CW, Blackburn EH. Identification of a specific telomere terminal transferase
691 activity in tetrahymena extracts. Cell. 1985;43(2):405-13. doi: 10.1016/0092-8674(85)90170-
692 9.
693 4. Weinrich SL, Pruzan R, Ma L, Ouellette M, Tesmer VM, Holt SE, et al.
694 Reconstitution of human telomerase with the template RNA component hTR and the catalytic
695 protein subunit hTRT. Nature Genetics. 1997;17(4):498-502. doi: 10.1038/ng1297-498.
696 5. Artandi SE, Chang S, Lee S-L, Alson S, Gottlieb GJ, Chin L, et al. Telomere
697 dysfunction promotes non-reciprocal translocations and epithelial cancers in mice. Nature.
698 2000;406(6796):641-5. doi: 10.1038/35020592.
699 6. Aubert G, Lansdorp PM. Telomeres and aging. Physiological reviews.
700 2008;88(2):557-79. doi: 10.1152/physrev.00026.2007. PubMed PMID: 18391173.
701 7. Keefe DL, Franco S, Liu L, Trimarchi J, Cao B, Weitzen S, et al. Telomere length
702 predicts embryo fragmentation after in vitro fertilization in women—Toward a telomere
703 theory of reproductive aging in women. American Journal of Obstetrics and Gynecology.
704 2005;192(4):1256-60. doi: 10.1016/j.ajog.2005.01.036.
705 8. Mu J, Wei LX. Telomere and telomerase in oncology. Cell research. 2002;12(1):1-7.
706 doi: 10.1038/sj.cr.7290104. PubMed PMID: 11942406.
707 9. Parkinson EK, Fitchett C, Cereser B. Dissecting the non-canonical functions of
708 telomerase. Cytogenetic and Genome Research. 2008;122(3-4):273-80. doi:
709 10.1159/000167813.
710 10. Teichroeb JH, Kim J, Betts DH. The role of telomeres and telomerase reverse
711 transcriptase isoforms in pluripotency induction and maintenance. RNA Biology.
712 2016;13(8):707-19. doi: 10.1080/15476286.2015.1134413.
713 11. Klapper W, Shin T, Mattson MP. Differential regulation of telomerase activity and
714 TERT expression during brain development in mice. Journal of neuroscience research.
715 2001;64(3):252-60. doi: 10.1002/jnr.1073. PubMed PMID: 11319769.
716 12. Maida Y, Yasukawa M, Furuuchi M, Lassmann T, Possemato R, Okamoto N, et al.
717 An RNA-dependent RNA polymerase formed by TERT and the RMRP RNA. Nature.
718 2009;461(7261):230-5. doi: 10.1038/nature08283. PubMed PMID: 19701182; PubMed
719 Central PMCID: PMC2755635.
720 13. Ahmed S, Passos JF, Birket MJ, Beckmann T, Brings S, Peters H, et al. Telomerase
721 does not counteract telomere shortening but protects mitochondrial function under oxidative
722 stress. Journal of cell science. 2008;121(Pt 7):1046-53. doi: 10.1242/jcs.019372. PubMed
723 PMID: 18334557.
724 14. Liu Z, Li Q, Li K, Chen L, Li W, Hou M, et al. Telomerase reverse transcriptase
725 promotes epithelial–mesenchymal transition and stem cell-like traits in cancer cells.
726 Oncogene. 2013;32(36):4203.
727 15. Gilson E, Ségal-Bendirdjian E. The telomere story or the triumph of an open-minded
728 research. Biochimie. 2010;92(4):321-6. doi: 10.1016/j.biochi.2009.12.014.

16. McClintock B. The Behavior in Successive Nuclear Divisions of a Chromosome Broken at Meiosis. PNAS. 1939;25(8):405-16. doi: 10.1073/pnas.25.8.405.
17. McClintock B. The stability of broken ends of chromosomes in Zea mays. Genetics. 1941;26(2):234.
18. Muller HJ. The remaking of chromosomes. Collecting net. 1938;13:181-98.
19. Szostak JW, Blackburn EH. Cloning yeast telomeres on linear plasmid vectors. Cell. 1982;29(1):245-55. doi: 10.1016/0092-8674(82)90109-x.
20. Annesley SJ, Fisher PR. Dictyostelium discoideum—a model for many reasons. Molecular and cellular biochemistry. 2009;329(1-2):73-91.
21. Maniak M. Dictyostelium as a model for human lysosomal and trafficking diseases. Seminars in Cell and Developmental Biology. 2011 ;22(1):114-9. doi: 10.1016/j.semcdb.2010.11.001.
22. Muller-Taubenberger A, Kortholt A, Eichinger L. Simple system--substantial share: the use of Dictyostelium in cell biology and molecular medicine. European journal of cell biology. 2013;92(2):45-53. doi: 10.1016/j.ejcb.2012.10.003. PubMed PMID: 23200106.
23. Williams JG. Dictyostelium Finds New Roles to Model. Genetics. 2010;185(3):717-26. doi: 10.1534/genetics.110.119297.
24. Williams RSB, Boeckeler K, Gräf R, Müller-Taubenberger A, Li Z, Isberg RR, et al. Towards a molecular understanding of human diseases using Dictyostelium discoideum. Trends in Molecular Medicine. 2006;12(9):415-24. doi: 10.1016/j.molmed.2006.07.003.
25. Hohl HR, Raper KB. Control of sorocarp size in the cellular slime mold Dictyostelium discoideum. Developmental Biology. 1964;9(1):137-53. doi: 10.1016/0012-1606(64)90018-1.
26. Brock DA, Buczynski G, Spann TP, Wood SA, Cardelli J, Gomer RH. A Dictystelium mutant with defective aggregate size determination. Development. 1996;122(9):2569-78. PubMed PMID: 8787732.
27. Brock DA, Ehrenman K, Ammann R, Tang Y, Gomer RH. Two components of a secreted cell number-counting factor bind to cells and have opposing effects on cAMP signal transduction in Dictyostelium. The Journal of biological chemistry. 2003;278(52):52262-72. doi: 10.1074/jbc.M309101200. PubMed PMID: 14557265.
28. Brock DA, Gomer RH. A cell-counting factor regulating structure size in Dictyostelium. Genes & development. 1999;13(15):1960-9. PubMed PMID: 10444594; PubMed Central PMCID: PMC316923.
29. Brock DA, Gomer RH. A secreted factor represses cell proliferation in Dictyostelium. Development. 2005;132(20):4553-62. doi: 10.1242/dev.02032. PubMed PMID: 16176950; PubMed Central PMCID: PMC4484793.
30. Brown JM, Firtel RA. Just the right size: cell counting in Dictyostelium. Trends in genetics : TIG. 2000;16(5):191-3. PubMed PMID: 10782107.
31. Gomer RH, Jang W, Brazill D. Cell density sensing and size determination. Development, growth & differentiation. 2011;53(4):482-94. doi: 10.1111/j.1440-169X.2010.01248.x. PubMed PMID: 21521184; PubMed Central PMCID: PMC3097309.
32. Jain R, Yuen IS, Taphouse CR, Gomer RH. A density-sensing factor controls development in Dictyostelium. Genes and development. 1992;6(3):390-400. doi: 10.1101/gad.6.3.390.
33. Jaiswal P, Soldati T, Thewes S, Baskar R. Regulation of aggregate size and pattern by adenosine and caffeine in cellular slime molds. BMC developmental biology. 2012;12:5. doi: 10.1186/1471-213X-12-5. PubMed PMID: 22269093; PubMed Central PMCID: PMC3341216.

34. Mehdy MC, Firtel RA. A secreted factor and cyclic AMP jointly regulate cell-type-specific gene expression in Dictyostelium discoideum. Molecular and Cellular Biology. 1985;5(4):705-13. doi: 10.1128/mcb.5.4.705.
35. Brock DA, Hatton RD, Giurgiutiu DV, Scott B, Ammann R, Gomer RH. The different components of a multisubunit cell number-counting factor have both unique and overlapping functions. Development. 2002;129(15):3657-68. PubMed PMID: 12117815.
36. Brock DA, Hatton RD, Giurgiutiu DV, Scott B, Jang W, Ammann R, et al. CF45-1, a secreted protein which participates in Dictyostelium group size regulation. Eukaryotic cell. 2003;2(4):788-97. PubMed PMID: 12912898; PubMed Central PMCID: PMC178340.
37. Bonner JT, Hoffman ME. Evidence for a Substance Responsible for the Spacing Pattern of Aggregation and Fruiting in the Cellular Slime Molds. Journal of Embryology and Experimental Morphology. 1963;11(3):571.
38. Loomis W. Dictyostelium discoideum: a developmental system. Cell. 2012. Elsevier.
39. Roisin-Bouffay C, Jang W, Caprette DR, Gomer RH. A precise group size in Dictyostelium is generated by a cell-counting factor modulating cell-cell adhesion. Molecular cell. 2000;6(4):953-9. PubMed PMID: 11090633.
40. Bakthavatsalam D, Brock DA, Nikravan NN, Houston KD, Hatton RD, Gomer RH. The secreted Dictyostelium protein CfaD is a chalone. Journal of cell science. 2008;121(Pt 15):2473-80. doi: 10.1242/jcs.026682. PubMed PMID: 18611962; PubMed Central PMCID: PMC2716657.
41. Iversen OH. Some theoretical considerations on chalones and the treatment of cancer: a review. Cancer research. 1970;30(5):1481-4.
42. Gaudet P, Fey P, Basu S, Bushmanova YA, Dodson R, Sheppard KA, et al. dictyBase update 2011: web 2.0 functionality and the initial steps towards a genome portal for the AmoebozoDDB0192195. Nucleic acids research. 2011;39(Database issue):D620-4. doi: 10.1093/nar/gkq1103. PubMed PMID: 21087999; PubMed Central PMCID: PMC3013695.
43. Eichinger L, Pachebat JA, Glockner G, Rajandream MA, Sucgang R, Berriman M, et al. The genome of the social amoeba Dictyostelium discoideum. Nature. 2005;435(7038):43-57. doi: 10.1038/nature03481. PubMed PMID: 15875012; PubMed Central PMCID: PMC1352341.
44. Sýkorová E, Fajkus J. Structure-function relationships in telomerase genes. Biology of the cell. 2009;101(7):375-406. doi: 10.1042/bc20080205.
45. Cong YS, Wright WE, Shay JW. Human telomerase and its regulation. Microbiology and molecular biology reviews : MMBR. 2002;66(3):407-25, table of contents. PubMed PMID: 12208997; PubMed Central PMCID: PMC120798.
46. Eichinger L, Noegel AA. Comparative genomics of Dictyostelium discoideum and Entamoeba histolytica. Current opinion in microbiology. 2005;8(5):606-11. doi: 10.1016/j.mib.2005.08.009. PubMed PMID: 16125444.
47. Shay JW, Zou Y, Hiyama E, Wright WE. Telomerase and cancer. Human molecular genetics. 2001;10(7):677-85. PubMed PMID: 11257099.
48. Cristofari G, Lingner J. Telomere length homeostasis requires that telomerase levels are limiting. The EMBO journal. 2006;25(3):565-74. doi: 10.1038/sj.emboj.7600952. PubMed PMID: 16424902; PubMed Central PMCID: PMC1383536.
49. Riedel V, Gerisch G, Muller E, Beug H. Defective cyclic adenosine-3', 5'-phosphate-phosphodiesterase regulation in morphogenetic mutants of Dictyostelium discoideum. Journal of molecular biology. 1973;74(4):573-85. PubMed PMID: 4354075.
50. Faure M, Podgorski GJ, Franke J, Kessin RH. Disruption of Dictyostelium discoideum morphogenesis by overproduction of cAMP phosphodiesterase. Proceedings of the National Academy of Sciences of the United States of America. 1988;85(21):8076-80. PubMed PMID: 2847151; PubMed Central PMCID: PMC282357.

827 51. Kesbeke F, Van Haastert PJ. Reduced cAMP secretion in Dictyostelium discoideum
828 mutant HB3. Developmental Biology. 1988;130(2):464-70. PubMed PMID: 2848740.
829 52. Mayanagi T, Amagai A, Maeda Y. DNG1, a Dictyostelium homologue of tumor
830 suppressor ING1 regulates differentiation of Dictyostelium cells. Cellular and molecular life
831 sciences : CMLS. 2005;62(15):1734-43. doi: 10.1007/s00018-005-4570-0. PubMed PMID:
832 16003496.
833 53. Sasaki K, Chae SC, Loomis WF, Iranfar N, Amagai A, Maeda Y. An immediate-early
834 gene, srsA: its involvement in the starvation response that initiates differentiation of
835 Dictyostelium cells. Differentiation. 2008;76(10):1093-103. doi: 10.1111/j.1432-
836 0436.2008.00298.x. PubMed PMID: 18673382.
837 54. Bolourani P, Spiegelman GB, Weeks G. Delineation of the roles played by RasG and
838 RasC in cAMP-dependent signal transduction during the early development of Dictyostelium
839 discoideum. Molecular biology of the cell. 2006;17(10):4543-50. doi: 10.1091/mbc.e05-11-
840 1019. PubMed PMID: 16885420; PubMed Central PMCID: PMC1635367.
841 55. Weijer CJ. Dictyostelium morphogenesis. Current opinion in genetics &
842 development. 2004;14(4):392-8. doi: 10.1016/j.gde.2004.06.006. PubMed PMID: 15261655.
843 56. Siegert F, Weijer CJ. Spiral and concentric waves organize multicellular
844 Dictyostelium mounds. Current biology : CB. 1995;5(8):937-43. PubMed PMID: 7583152.
845 57. El-Brolosy MA, Stainier DYR. Genetic compensation: A phenomenon in search of
846 mechanisms. PLOS Genetics. 2017;13(7):e1006780. doi: 10.1371/journal.pgen.1006780.
847 58. Tautz D. Problems and paradigms: Redundancies, development and the flow of
848 information. BioEssays. 1992;14(4):263-6. doi: doi:10.1002/bies.950140410.
849 59. Darmon M, Brachet P, Da Silva LH. Chemotactic signals induce cell differentiation in
850 Dictyostelium discoideum. Proceedings of the National Academy of Sciences of the United
851 States of America. 1975;72(8):3163-6. PubMed PMID: 171655; PubMed Central PMCID:
852 PMC432941.
853 60. Mann SK, Firtel RA. Cyclic AMP regulation of early gene expression in
854 Dictyostelium discoideum: mediation via the cell surface cyclic AMP receptor. Molecular
855 and Cellular Biology. 1987;7(1):458-69. PubMed PMID: 3031475; PubMed Central PMCID:
856 PMC365089.
857 61. Van Haastert PJ, Kien E. Binding of cAMP derivatives to Dictyostelium discoideum
858 cells. Activation mechanism of the cell surface cAMP receptor. The Journal of biological
859 chemistry. 1983;258(16):9636-42. PubMed PMID: 6309778.
860 62. Theibert A, Devreotes PN. Adenosine and its derivatives inhibit the cAMP signaling
861 response in Dictyostelium discoideum. Developmental Biology. 1984;106(1):166-73.
862 PubMed PMID: 6092178.
863 63. Brenner M, Thoms SD. Caffeine blocks activation of cyclic AMP synthesis in
864 Dictyostelium discoideum. Developmental Biology. 1984;101(1):136-46. PubMed PMID:
865 6319207.
866 64. Buracco S, Peracino B, Andreini C, Bracco E, Bozzaro S. Differential Effects of Iron,
867 Zinc, and Copper on Dictyostelium discoideum Cell Growth and Resistance to Legionella
868 pneumophila. Frontiers in cellular and infection microbiology. 2017;7:536. doi:
869 10.3389/fcimb.2017.00536. PubMed PMID: 29379774; PubMed Central PMCID:
870 PMC5770829.
871 65. Coates JC, Harwood AJ. Cell-cell adhesion and signal transduction during
872 Dictyostelium development. Journal of cell science. 2001;114(Pt 24):4349-58. PubMed
873 PMID: 11792801.
874 66. Suess PM, Watson J, Chen W, Gomer RH. Extracellular polyphosphate signals
875 through Ras and Akt to prime Dictyostelium discoideum cells for development. Journal of

876 cell science. 2017;130(14):2394-404. doi: 10.1242/jcs.203372. PubMed PMID: 28584190;
877 PubMed Central PMCID: PMC5536921.
878 67. Jang W, Chiem B, Gomer RH. A secreted cell number counting factor represses
879 intracellular glucose levels to regulate group size in dictyostelium. The Journal of biological
880 chemistry. 2002;277(42):39202-8. doi: 10.1074/jbc.M205635200. PubMed PMID:
881 12161440.
882 68. Heidel AJ, Lawal HM, Felder M, Schilde C, Helps NR, Tunggal B, et al. Phylogeny-
883 wide analysis of social amoeba genomes highlights ancient origins for complex intercellular
884 communication. Genome research. 2011;21(11):1882-91. doi: 10.1101/gr.121137.111.
885 PubMed PMID: 21757610; PubMed Central PMCID: PMC3205573.
886 69. Bürglin TR, Affolter M. Homeodomain proteins: an update. Chromosoma.
887 2016;125(3):497-521. Epub 2015/10/13. doi: 10.1007/s00412-015-0543-8. PubMed PMID:
888 26464018.
889 70. Gehring WJ, Affolter M, Bürglin T. Homeodomain proteins. Annual Review of
890 Biochemistry. 1994;63(1):487-526. doi: 10.1146/annurev.bi.63.070194.002415.
891 71. Fey P, Kowal AS, Gaudet P, Pilcher KE, Chisholm RL. Protocols for growth and
892 development of Dictyostelium discoideum. Nature protocols. 2007;2(6):1307-16. doi:
893 10.1038/nprot.2007.178. PubMed PMID: 17545967.
894 72. Damm K, Hemmann U, Garin-Chesa P, Hauel N, Kauffmann I, Priepke H, et al. A
895 highly selective telomerase inhibitor limiting human cancer cell proliferation. The EMBO
896 journal. 2001;20(24):6958-68. doi: 10.1093/emboj/20.24.6958. PubMed PMID: 11742973;
897 PubMed Central PMCID: PMC125790.
898 73. Seimiya H, Oh-hara T, Suzuki T, Naasani I, Shimazaki T, Tsuchiya K, et al. Telomere
899 shortening and growth inhibition of human cancer cells by novel synthetic telomerase
900 inhibitors MST-312, MST-295, and MST-1991. Molecular cancer therapeutics.
901 2002;1(9):657-65. PubMed PMID: 12479362.
902 74. Gomer RH, Yuen IS, Firtel RA. A secreted 80 x 10(3) Mr protein mediates sensing of
903 cell density and the onset of development in Dictyostelium. Development. 1991;112(1):269-
904 78. PubMed PMID: 1663029.
905 75. Tang L, Gao T, McCollum C, Jang W, Vicker MG, Ammann RR, et al. A cell
906 number-counting factor regulates the cytoskeleton and cell motility in Dictyostelium.
907 Proceedings of the National Academy of Sciences of the United States of America.
908 2002;99(3):1371-6. doi: 10.1073/pnas.022516099. PubMed PMID: 11818526; PubMed
909 Central PMCID: PMC122197.
910 76. Desbarats L, Brar SK, Siu CH. Involvement of cell-cell adhesion in the expression of
911 the cell cohesion molecule gp80 in Dictyostelium discoideum. Journal of cell science.
912 1994;107 (Pt 6):1705-12. PubMed PMID: 7962211.
913 77. Fey P, Stephens S, Titus MA, Chisholm RL. SadA, a novel adhesion receptor in
914 Dictyostelium. The Journal of cell biology. 2002;159(6):1109-19. doi:
915 10.1083/jcb.200206067. PubMed PMID: 12499361; PubMed Central PMCID:
916 PMC2173991.
917 78. Woznica D, Knecht DA. Under-agarose chemotaxis of Dictyostelium discoideum.
918 Methods in molecular biology. 2006;346:311-25. doi: 10.1385/1-59745-144-4:311. PubMed
919 PMID: 16957299.
920 79. Pilcher KE, Gaudet P, Fey P, Kowal AS, Chisholm RL. A general purpose method for
921 extracting RNA from Dictyostelium cells. Nature protocols. 2007;2(6):1329-32. doi:
922 10.1038/nprot.2007.191. PubMed PMID: 17545970.
923 80. Schmittgen TD, Livak KJ. Analyzing real-time PCR data by the comparative C(T)
924 method. Nature protocols. 2008;3(6):1101-8. PubMed PMID: 18546601.

81. Aschar-Sobbi R, Abramov AY, Diao C, Kargacin ME, Kargacin GJ, French RJ, et al. High sensitivity, quantitative measurements of polyphosphate using a new DAPI-based approach. Journal of fluorescence. 2008;18(5):859-66. doi: 10.1007/s10895-008-0315-4. PubMed PMID: 18210191.
82. Van Haastert PJ. Sensory adaptation of Dictyostelium discoideum cells to chemotactic signals. The Journal of cell biology. 1983;96(6):1559-65. PubMed PMID: 6304109; PubMed Central PMCID: PMC2112430.
83. Chisholm RL, Firtel RA. Insights into morphogenesis from a simple developmental system. Nature reviews Molecular cell biology. 2004;5(7):531-41. doi: 10.1038/nrm1427. PubMed PMID: 15232571.
84. Wang B, Kuspa A. Dictyostelium development in the absence of cAMP. Science. 1997;277(5323):251-4. PubMed PMID: 9211856.
85. Rutherford CL, Overall DF, Ubeidat M, Joyce BR. Analysis of 5' nucleotidase and alkaline phosphatase by gene disruption in Dictyostelium. Genesis. 2003;35(4):202-13. doi: 10.1002/gene.10185. PubMed PMID: 12717731.
86. Garcia GL, Rericha EC, Heger CD, Goldsmith PK, Parent CA. The group migration of Dictyostelium cells is regulated by extracellular chemoattractant degradation. Molecular biology of the cell. 2009;20(14):3295-304. doi: 10.1091/mbc.E09-03-0223. PubMed PMID: 19477920; PubMed Central PMCID: PMC2710833.
87. Bader S, Kortholt A, Snippe H, Van Haastert PJ. DdPDE4, a novel cAMP-specific phosphodiesterase at the surface of dictyostelium cells. The Journal of biological chemistry. 2006;281(29):20018-26. doi: 10.1074/jbc.M600040200. PubMed PMID: 16644729.
88. Gomer RH, Yuen IS, Firtel RA. A secreted 80 × 10(3) Mr protein mediates sensing of cell density and the onset of development in Dictyostelium. Development. 1991;112(1):269.
89. Loomis WF. Cell signaling during development of Dictyostelium. Developmental biology. 2014;391(1):1-16. doi: 10.1016/j.ydbio.2014.04.001.
90. Ma H, Gamper M, Parent C, Firtel RA. The Dictyostelium MAP kinase kinase DdMEK1 regulates chemotaxis and is essential for chemoattractant-mediated activation of guanylyl cyclase. The EMBO journal. 1997;16(14):4317-32. PubMed PMID: 9250676; PubMed Central PMCID: PMC1170058.
91. Schaap P, Wang M. Interactions between adenosine and oscillatory cAMP signaling regulate size and pattern in Dictyostelium. Cell. 1986;45(1):137-44. PubMed PMID: 3006924.
92. Gao T, Knecht D, Tang L, Hatton RD, Gomer RH. A cell number counting factor regulates Akt/protein kinase B to regulate Dictyostelium discoideum group size. Eukaryotic cell. 2004;3(5):1176-84. doi: 10.1128/EC.3.5.1176-1184.2004. PubMed PMID: 15470246; PubMed Central PMCID: PMC522607.
93. Swaney KF, Huang CH, Devreotes PN. Eukaryotic chemotaxis: a network of signaling pathways controls motility, directional sensing, and polarity. Annual review of biophysics. 2010;39:265-89. doi: 10.1146/annurev.biophys.093008.131228. PubMed PMID: 20192768; PubMed Central PMCID: PMC4364543.
94. Varnum B, Soll DR. Effects of cAMP on single cell motility in Dictyostelium. The Journal of cell biology. 1984;99(3):1151-5. PubMed PMID: 6088555; PubMed Central PMCID: PMC2113391.
95. Jang W, Gomer RH. Exposure of cells to a cell number-counting factor decreases the activity of glucose-6-phosphatase to decrease intracellular glucose levels in Dictyostelium discoideum. Eukaryotic cell. 2005;4(1):72-81. doi: 10.1128/EC.4.1.72-81.2005. PubMed PMID: 15643062; PubMed Central PMCID: PMC544156.
96. Jang W, Gomer RH. A protein in crude cytosol regulates glucose-6-phosphatase activity in crude microsomes to regulate group size in Dictyostelium. The Journal of

biological chemistry. 2006;281(24):16377-83. doi: 10.1074/jbc.M509995200. PubMed PMID: 16606621; PubMed Central PMCID: PMC4486306.
97. Varnum B, Edwards KB, Soll DR. The developmental regulation of single-cell motility in Dictyostelium discoideum. Developmental Biology. 1986;113(1):218-27. PubMed PMID: 3943662.
98. Tang L, Ammann R, Gao T, Gomer RH. A cell number-counting factor regulates group size in Dictyostelium by differentially modulating cAMP-induced cAMP and cGMP pulse sizes. The Journal of biological chemistry. 2001;276(29):27663-9. doi: 10.1074/jbc.M102205200. PubMed PMID: 11371560.
99. Beug H, Katz FE, Gerisch G. Dynamics of antigenic membrane sites relating to cell aggregation in Dictyostelium discoideum. The Journal of cell biology. 1973;56(3):647-58. PubMed PMID: 4631665; PubMed Central PMCID: PMC2108928.
100. Yang C, Brar SK, Desbarats L, Siu CH. Synthesis of the Ca(2+)-dependent cell adhesion molecule DdCAD-1 is regulated by multiple factors during Dictyostelium development. Differentiation; research in biological diversity. 1997;61(5):275-84. doi: 10.1046/j.1432-0436.1997.6150275.x. PubMed PMID: 9342838.
101. Tarantola M, Bae A, Fuller D, Bodenschatz E, Loomis W. Cell Substratum Adhesion during Early Development of Dictyostelium discoideum. PLoS One. 2014;9(9):e106574. doi: 10.1371/journal.pone.0106574.
102. Coates JC, Harwood AJ. Cell-cell adhesion and signal transduction during Dictyostelium development. Journal of cell science. 2001;114(24):4349-58.

Figure legends:

Fig 1. Some of the events, processes and regulators of growth and development in *D. discoideum*. This figure depicts only a small number of the hypothesized regulatory pathways of *Dictyostelium* growth and development, focusing on those that were examined experimentally in this study. A line ending in an arrowhead suggests that the first element directly or indirectly promotes the activity or levels of the second; inhibition is suggested by a line ending in a cross-bar. Published works that report on the nature of each pathway within the network are as follows: a[29], [40]; b[29]; c[66]; d[52], [53], [54]; e[61], [82], [83], [84]; f[85]; g [86], [87]; h[88-90]; i[91], [33]; j[77]; k[92], [93], [94]; l[26], [39]; m[27]; n[35]; o[95], [96]; p[67]; q[67], [75]; r[67]; s[97]; t[75]; u[65]; v[98], [39]; w[99], [100]; x[66]; y[101].

Fig 2. *Tert* expression during growth and development in *D. discoideum*. *Tert* is a single copy gene in *Dictyostelium.* Total RNA was extracted from *Dictyostelium* strain AX2 during vegetative growth and development. To analyze *tert* expression, qRT-PCR was carried out and fold change was calculated. *rnlA* was used as a control. Time points are shown in hours (bottom). qRT-PCR was carried out thrice. Error bars represent the mean and SEM.

Fig 3. Developmental phenotype of *tert* KO. (A) AX2 and *tert* KO cells plated on 1% non-nutrient KK_2 agar plates at a density of $5x10^5$ cells/cm^2 were incubated in a dark, moist chamber. After 16 hours, large aggregate streams were formed in *tert* KO. The time points in hours are shown at the top. Scale bar-0.5 mm. (B) Quantitative measurement of aggregation. The number of aggregates was counted per centimetre square area. Level of significance is indicated as *p<0.05, **p<0.01, ***p<0.001, and ****p<0.0001.

Fig 4. (A) Overexpression of TERT (act15/gfp::*tert)* rescued *tert* KO phenotype. Scale bar-0.5 mm. (B) AX2 cells treated with 100nM BIBR 1532 and 250 nM MST 312 phenocopied the *tert* KO streaming phenotype. The time points in hours are shown at the top. Scale bar-0.5 mm.

Fig 5. *Tert* regulates the levels of CF. qRT-PCR of (A) *countin* and (B) *smlA* during aggregation in AX2, *tert* KO and *tert* KO [act15/gfptert]. *rnlA* was used as mRNA amplification control. Level of significance is indicated as *p<0.05, **p<0.01, ***p<0.001, and ****p<0.0001. (C) Western blots with anti-countin antibodies. The gels were stained with Coomassie to show equal loading. (D) *Countin* KO cells were developed in the presence of *tert* KO conditioned media or BIBR1532. Scale bar- 0.5 mm. D) Cells were starved and developed with anti-countin, CF50, CF45, AprA and CfaD antibodies (1:300 dilution). Addition of anti-countin and anti-CF50 antibodies rescued *tert* KO group size defect. Scale bar- 0.5 mm.

Fig 6. *Tert* regulates the levels of CF. (A) *Countin* KO cells were developed in the presence of *tert* KO conditioned media or BIBR1532. Scale bar- 0.5 mm. (B) Development in the presence of conditioned medium. *Tert* KO-CM induced stream breaking in AX2. (C) Reconstitution of AX2 in 1:9 ratio with *tert* KO did not rescue the stream breaking. Scale bar- 0.5 mm.

Fig 7. Development of other Dictyostelid species in the presence of *tert* KO conditioned medium. *tert* KO-CM did not alter the group size of other Dictyostelids. Scale bar- 0.5 mm.

Fig 8. Effect of glucose on *tert* KO aggregate size. (A) Glucose levels during aggregation. (B) Wild-type AX2 and *tert* KO cells were developed in the presence of 1 mM glucose. Glucose rescues the streaming defect of *tert* KO. Scale bar- 0.5 mm. Level of significance is indicated as *p<0.05, **p<0.01, ***p<0.001, and ****p<0.0001.

Fig 9. Cells were starved and developed with AprA and CfaD antibodies (1:300 dilution). Scale bar- 0.5 mm.

Fig 10. cAMP wave generating centres. Optical density wave images depicting wave generating centres in AX2, *tert* KO and rescue strain are shown. AX2 and rescue strain has a single wave generating centre, whereas *tert* KO has multiple wave generating centres in a single aggregate. Scale bar- 1 mm.

Fig 11: Delayed development in *tert* KO. (A-F) qRT-PCR of genes involved in the cAMP relay. Down-regulation of genes involved in the cAMP relay in *tert* KO. Fold change in mRNA expression is relative to AX2 at the indicated time points. *rnlA* is used as mRNA amplification control.

Fig 12. Defective cAMP relay of *tert* KO. cAMP relay and expression of *acaA, carA, pde4, pdsA* in *tert* KO during (A) aggregation and (B) stream breaking. Fold change in mRNA expression is relative to AX2 at the indicated time points. *rnlA* was used as mRNA

amplification control. cAMP levels in *tert* KO during (C) 8 h of development in AX2 and *tert* KO, (D) aggregation, (E) stream breaking. Level of significance is indicated as *p<0.05, **p<0.01, ***p<0.001, and ****p<0.0001.

Fig 13. Defective cAMP chemotaxis of *tert* KO. Under-agarose cAMP chemotaxis assay in response to 10µM cAMP. (A) Average chemotaxis speed in response to cAMP. (B) directionality of chemotaxing cells and (C) chemotaxis index are shown. The graph represents the mean and SEM of 3 independent experiments.

Fig 14. cAMP sensing in *tert* KO. (A) Wild-type and *tert* KO cells were starved for 1 hour and pulsed every 6 min with 50 nM cAMP for 4 h. Cells were then resuspended in BSS and seeded at a density of $1x10^5$ cells/ml, and observed under a microscope. (B) Wild-type and *tert* KO cells were washed in BSS, seeded at a density of $1x10^5$ cells/ ml, and incubated in BSS or BSS + 5 mM 8-Br-cAMP for 5 h. Cells were washed and then observed under a microscope. Scale bar- 100 µm.

Fig 15. Effect of adenosine on aggregate size. (A) qRT-PCR of 5'NT. Fold change in mRNA expression is relative to AX2 at indicated time points. *rnlA* is used as mRNA amplification control. (B) Quantification of adenosine levels. Level of significance is indicated as *p<0.05, **p<0.01, ***p<0.001, and ****p<0.0001. (C) Cells were developed in the presence of 1mM caffeine; *tert* KO streaming defect was rescued. Scale bar- 0.5 mm.

Fig 16. Disruption of *tert* affects cell substratum adhesion. Cells were plated at a density of $1x10^5$ cells/ml, grown overnight, in an orbital shaker. Floating and attached cells were counted and percentage adhesion was plotted versus rotation speed. Both AX2 and *tert* KO exhibited a sheer force-dependent decrease in substratum adhesion and *tert* KO exhibited significantly reduced adhesion compared to AX2 cells.

Fig 17. **Disruption of *tert* affects cell adhesion.** qRT-PCR of (A) *csaA* and (B) *cadA. rnlA* was used as mRNA amplification control. Wild-type and *tert* KO cells were starved in Sorensen phosphate buffer at 150 rpm and 22 ºC. Samples were collected at the start of the assay and at one-hour time points after 4 h of starvation. Percentage of cell adhesion plotted over time. (C) EDTA resistant cell-cell adhesion, (D) EDTA sensitive cell-cell adhesion. Level of significance is indicated as *p<0.05, **p<0.01, ***p<0.001, and ****p<0.0001.

Fig 18. Rescue of delay by added wild-type cells. Wild-type AX2 and *tert* KO were reconstituted at 1:9, 2:8 and 1:1 ratio. Developmental delay of *tert* KO was rescued by AX2 at 1:1 ratio. Scale bar- 0.5 mm.

Fig 19. Polyphosphate levels were low in the *tert* KO. Polyphosphate levels in conditioned media of AX2 and *tert* KO. Level of significance is indicated as *p<0.05, **p<0.01, ***p<0.001, and ****p<0.0001.

Fig 20. Some of the possible targets of *tert*/TERT in development of *D. discoideum*, as indicated by this study. This work, the first functional study of a telomerase in *Dictyostelium*, revealed that TERT influenced many previously reported developmental processes and pathways. The dashed lines represent effects previously unreported, involving multiples phases of the life-cycle. Adenosine, however, was found to provide negative feedback on *tert* expression. The depictions of life-cycle changes were drawn by the authors, based on images in [102], and adapted by kind permission of the Journal of Cell Science.

Supporting information

S1 Fig. Schematic representation of the different functional domains of TERT identified with SMART analysis. TERT protein contains the following domains: reverse transcriptase and RNA binding domain.

S2 Fig. Telomerase activity assay. TRAP assay was performed for AX2 and *tert* KO. Human cell lines HEK and HeLa were used as positive controls.

S3 Fig. Changing cell density and its effect on development. Development assay at different cell density ($2x10^4$ cells/cm^2 to $2x10^6$ cells/cm^2). AX2 cells aggregate even at a cell density below $2x10^4$ cells/cm^2, but *tert* KO fails to aggregate at such a density. *Tert* KO phenotype was not rescued even at higher cell density ($2x10^6$ cells/cm^2).

S4 Fig. Effect of adenosine on aggregate size in *D. discoideum*. A) qRT-PCR of 5'NT during stream breaking. Fold change in mRNA expression is relative to AX2 at the indicated time points. *rnlA* is used as mRNA amplification control. B) Quantification of adenosine levels during stream breaking. Level of significance is indicated as *p<0.05, **p<0.01, ***p<0.001, and ****p<0.0001.

S5 Fig. *Tert* levels in adenosine treated cells.

S6 Fig. Quantification of iron. Iron levels were quantified by ICP-MS. Level of significance is indicated as *p<0.05, **p<0.01, ***p<0.001, and ****p<0.0001.

S1 Table. Primers used for TERT overexpression vector construction.

S2 Table. Primers used for real-time PCR.

Video 1. Timelapse video of AX2 development.

Video 2. Timelapse video of *tert* KO development.

Video 3. Timelapse video of *tert* KO (act15/gfp::*tert*) development.

Video 4. Timelapse video of cAMP wave propagation in AX2.

Video 5. Timelapse video of cAMP wave propagation in *tert* KO.

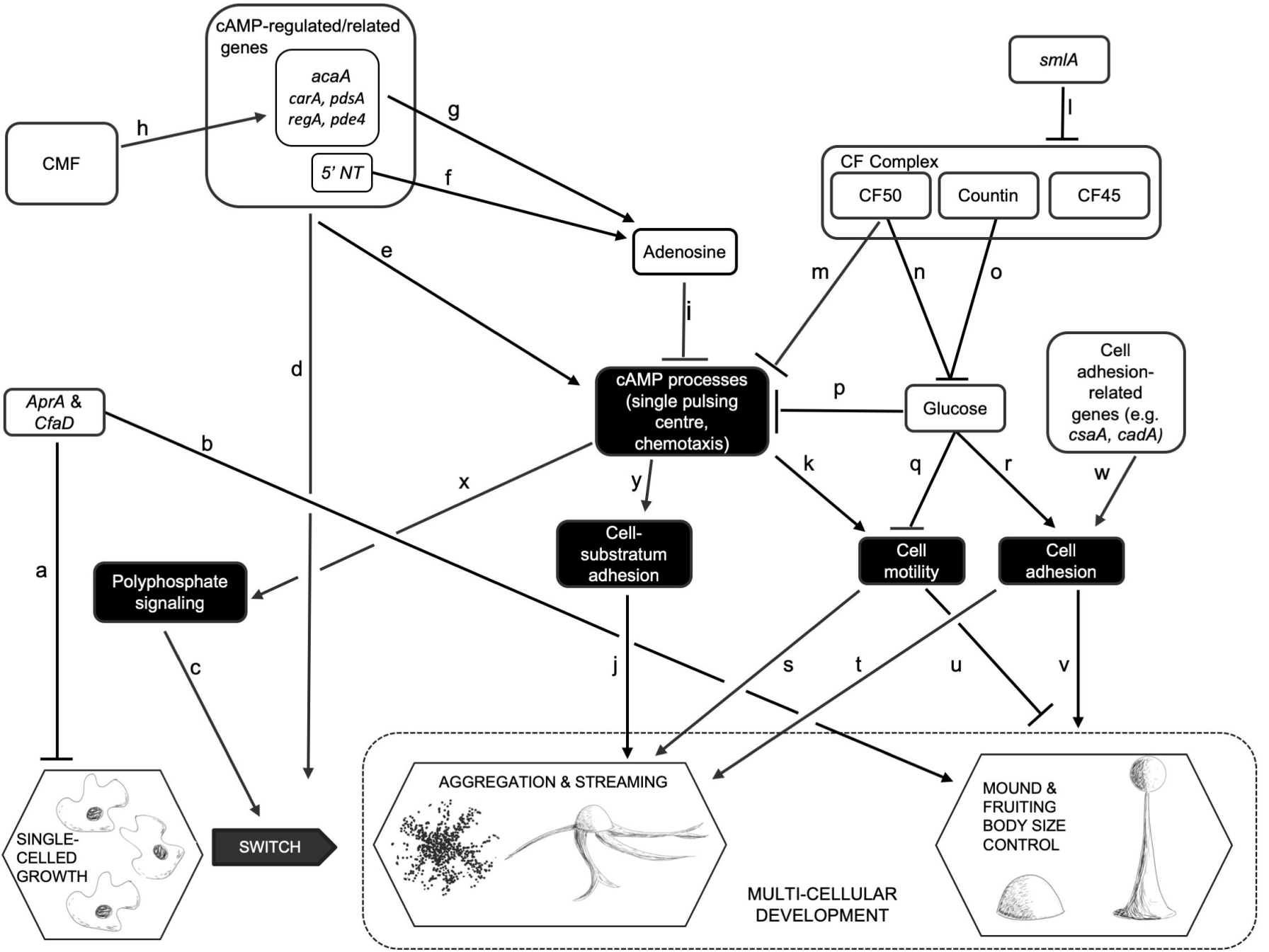
cAMP-regulated/related genes
acaA
carA, pdsA
regA, pde4
5' NT
CMF
h
g
f
e
d
smlA
l
CF Complex
CF50
Countin
CF45
Adenosine
i
m
n
o
cAMP processes (single pulsing centre, chemotaxis)
p
Glucose
Cell adhesion-related genes (e.g. csaA, cadA)
AprA & CfaD
b
x
y
k
q
r
w
a
Polyphosphate signaling
Cell-substratum adhesion
Cell motility
Cell adhesion
c
j
s
t
u
v
SINGLE-CELLED GROWTH
SWITCH
AGGREGATION & STREAMING
MOUND & FRUITING BODY SIZE CONTROL
MULTI-CELLULAR DEVELOPMENT

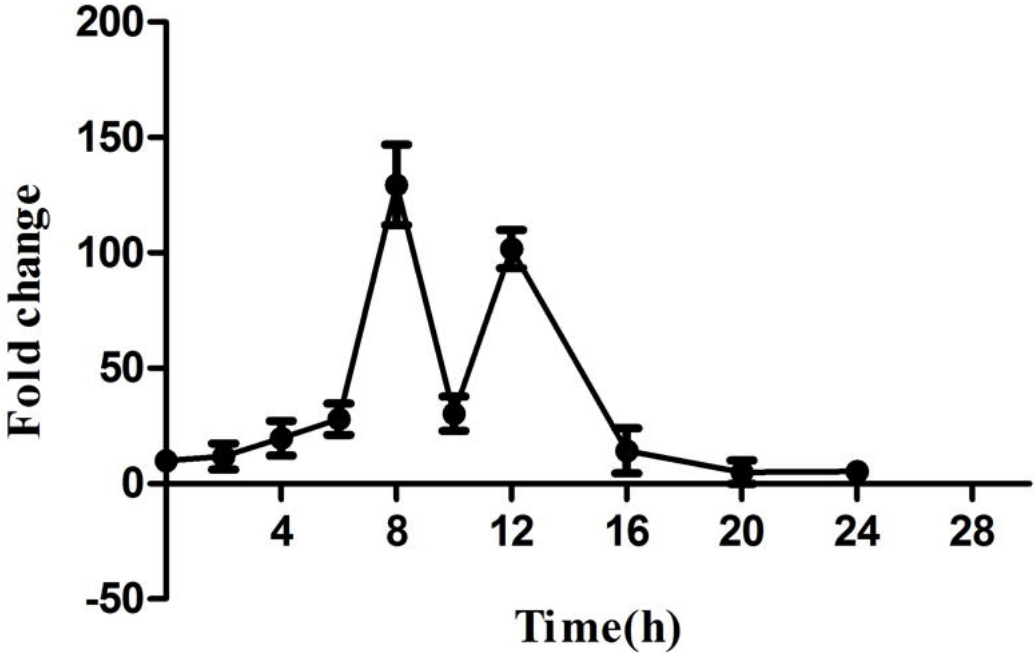
200
150
100
50
0
-50
Fold change
4
8
12
16
20
24
28
Time(h)

A

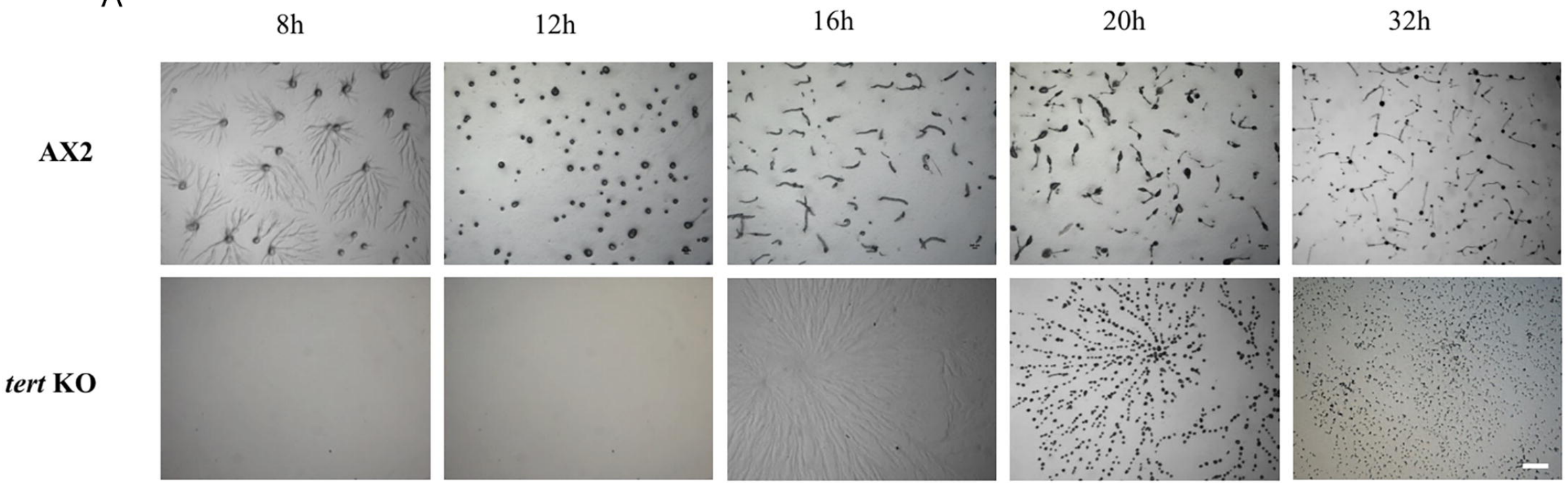
8h
12h
16h
20h
32h
AX2
tert KO

B

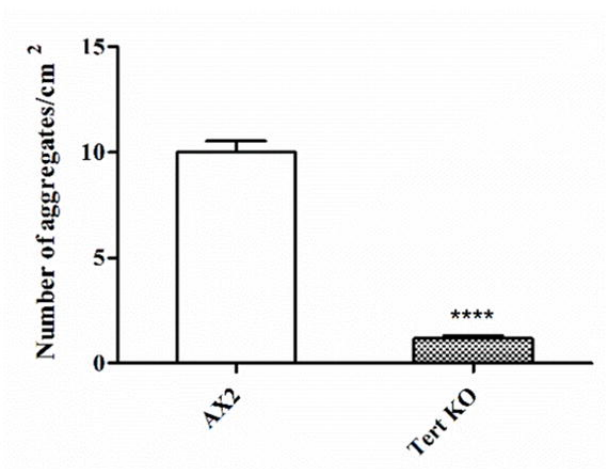
Number of aggregates/cm 2
15
10
5
0
****
AX2
Tert KO

A

8h

12h

AX2[act15/gfp::*tert*]

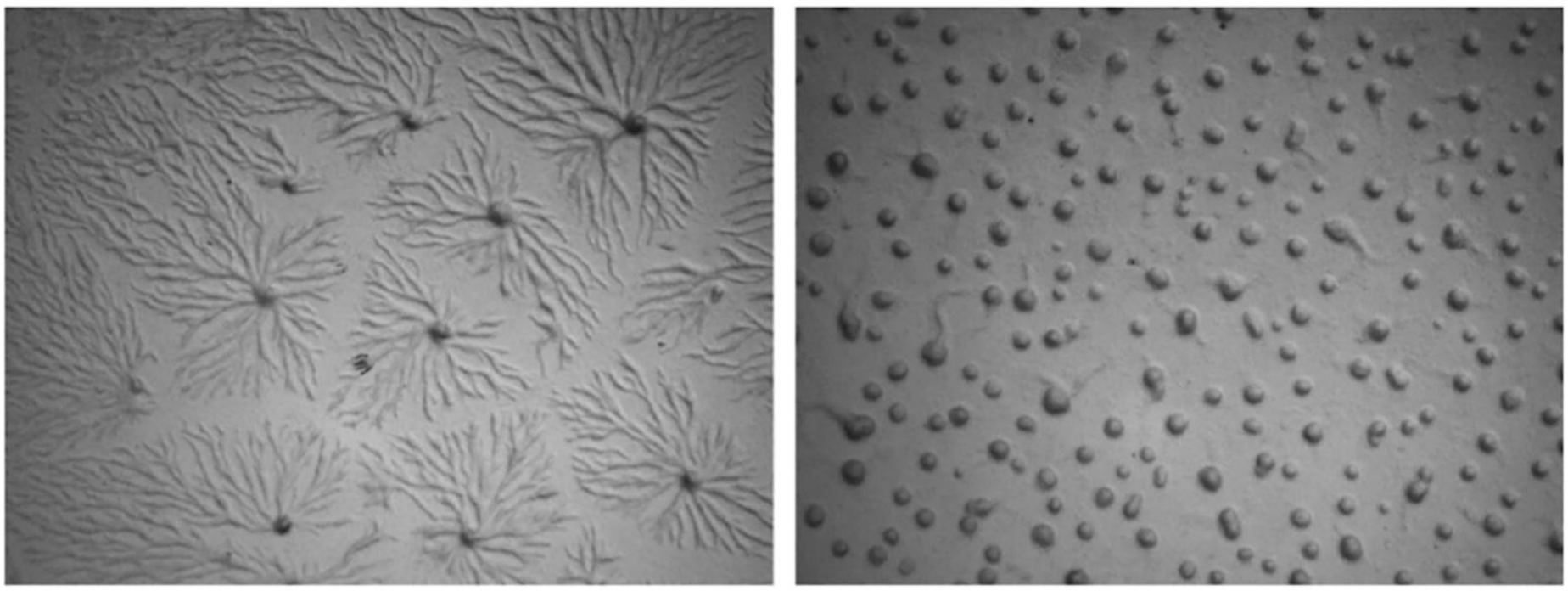

tert KO[act15/gfp::*tert*]

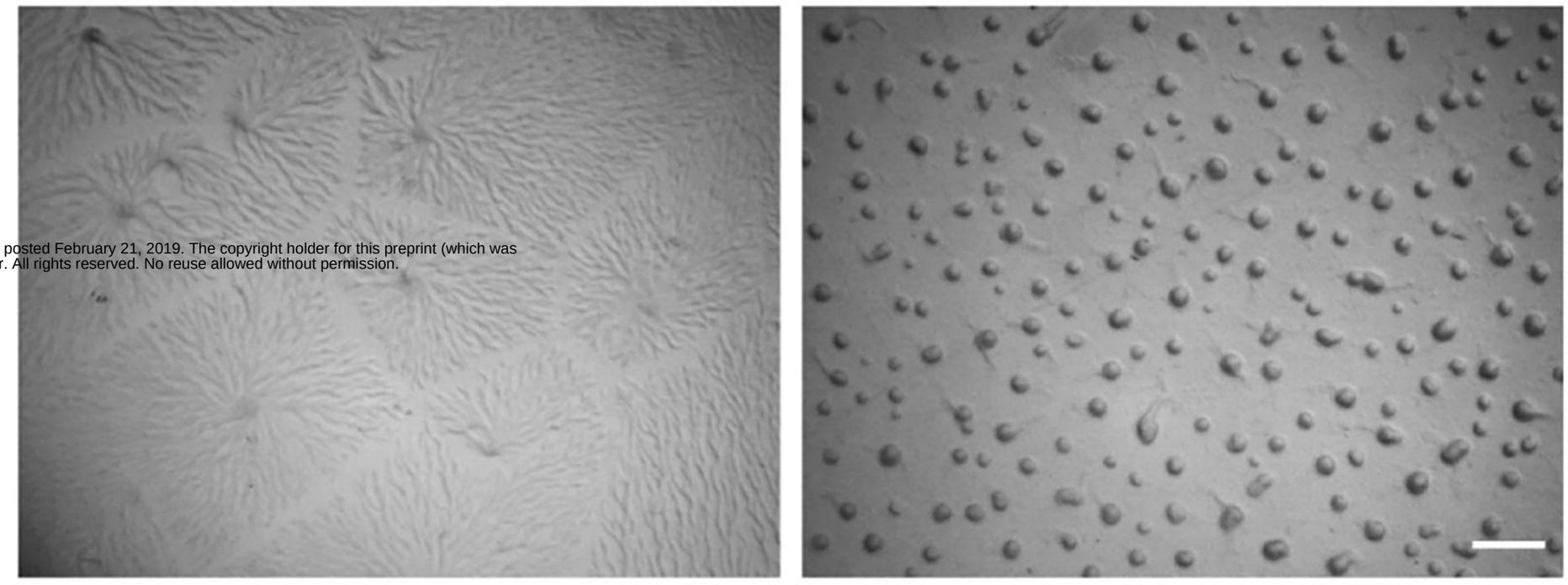

B

8h

12h

16h

20h

32h

AX2

AX2+ 100nM BIBR

AX2+ 250nM MST 312

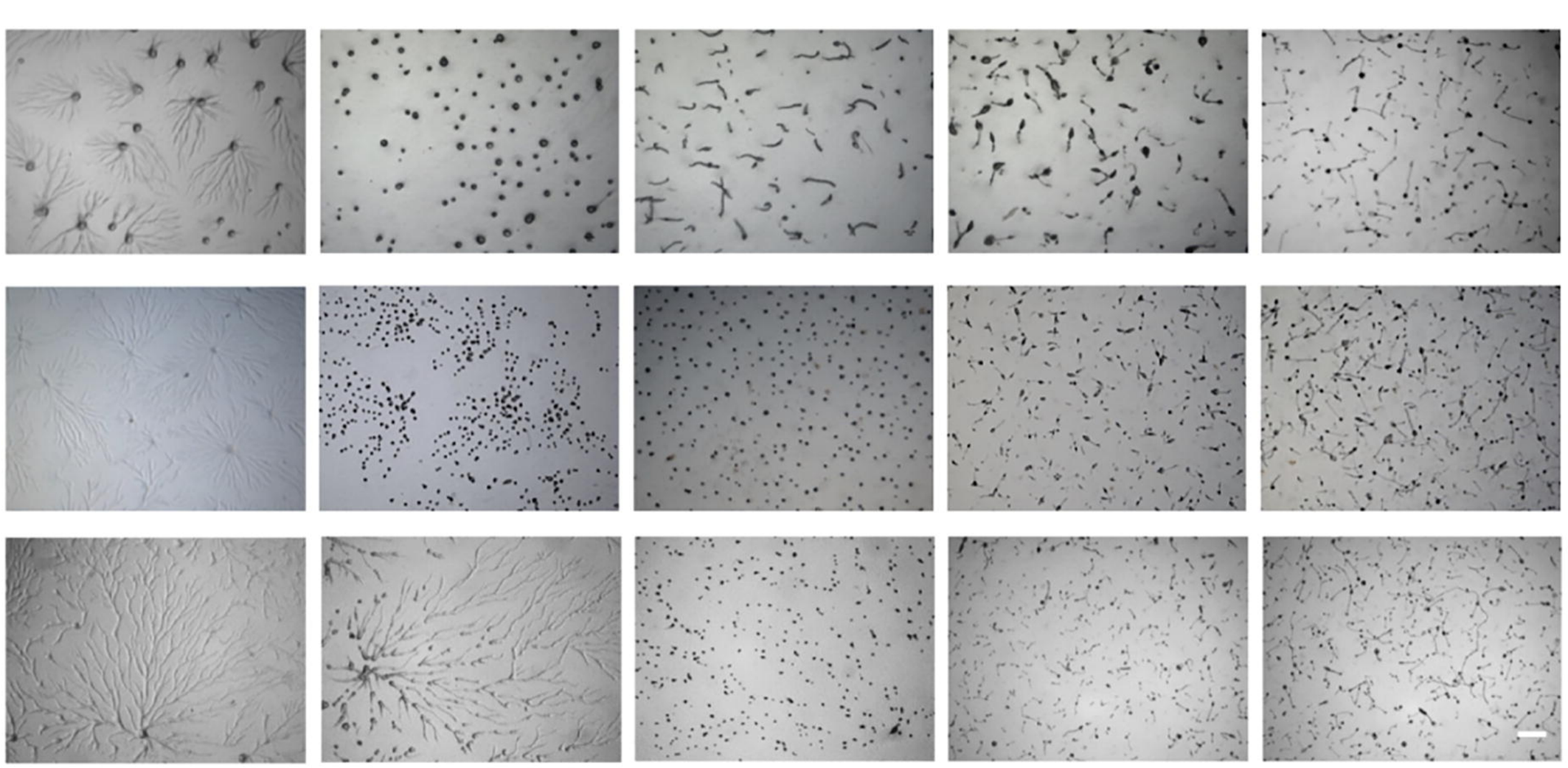

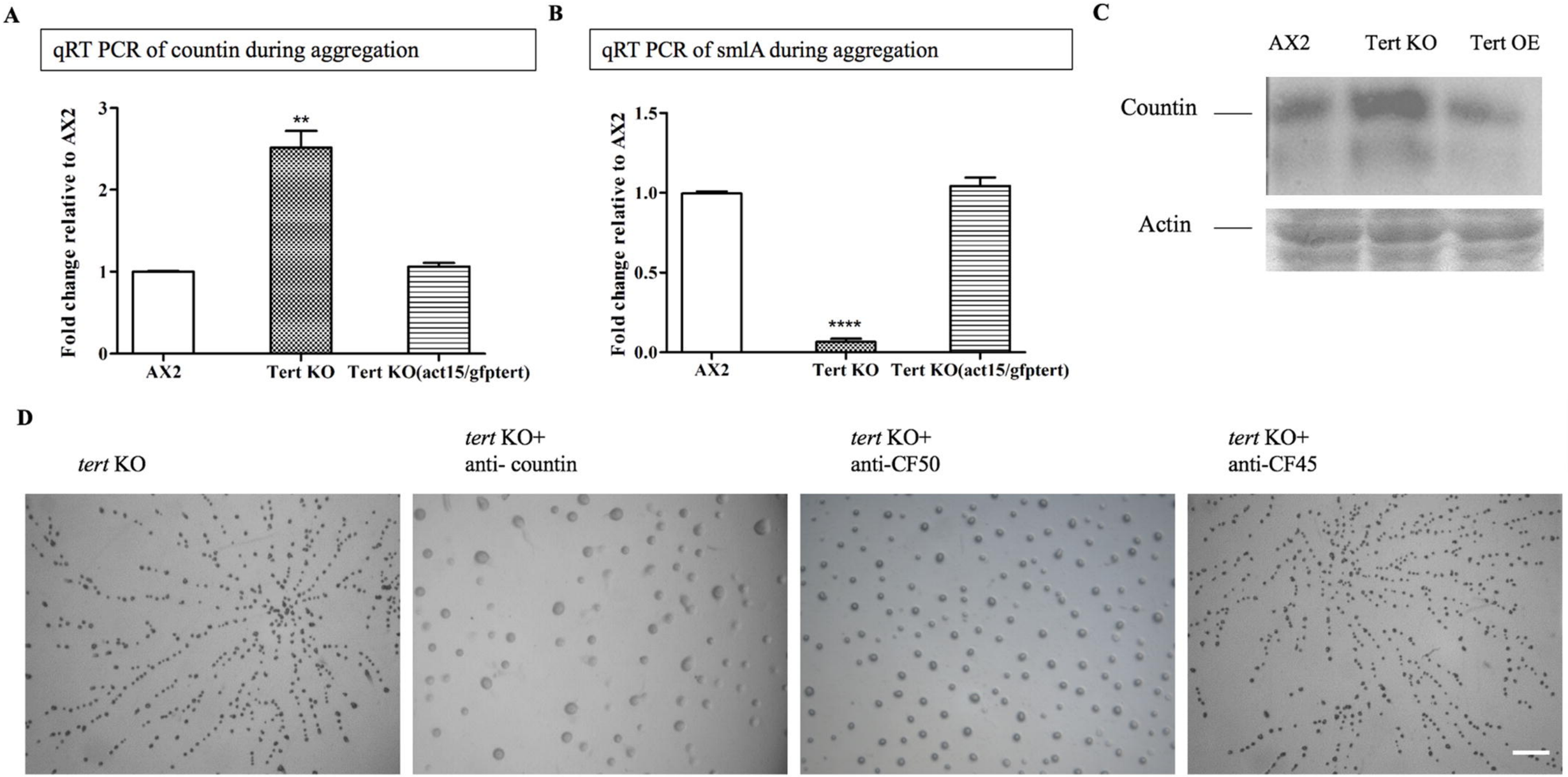
A
qRT PCR of countin during aggregation
Fold change relative to AX2
3
2
1
0
**
AX2
Tert KO
Tert KO(act15/gfptert)
B
qRT PCR of smlA during aggregation
Fold change relative to AX2
1.5
1.0
0.5
0.0
****
AX2
Tert KO
Tert KO(act15/gfptert)
C
AX2
Tert KO
Tert OE
Countin
Actin
D
tert KO
tert KO+
anti- countin
tert KO+
anti-CF50
tert KO+
anti-CF45

A

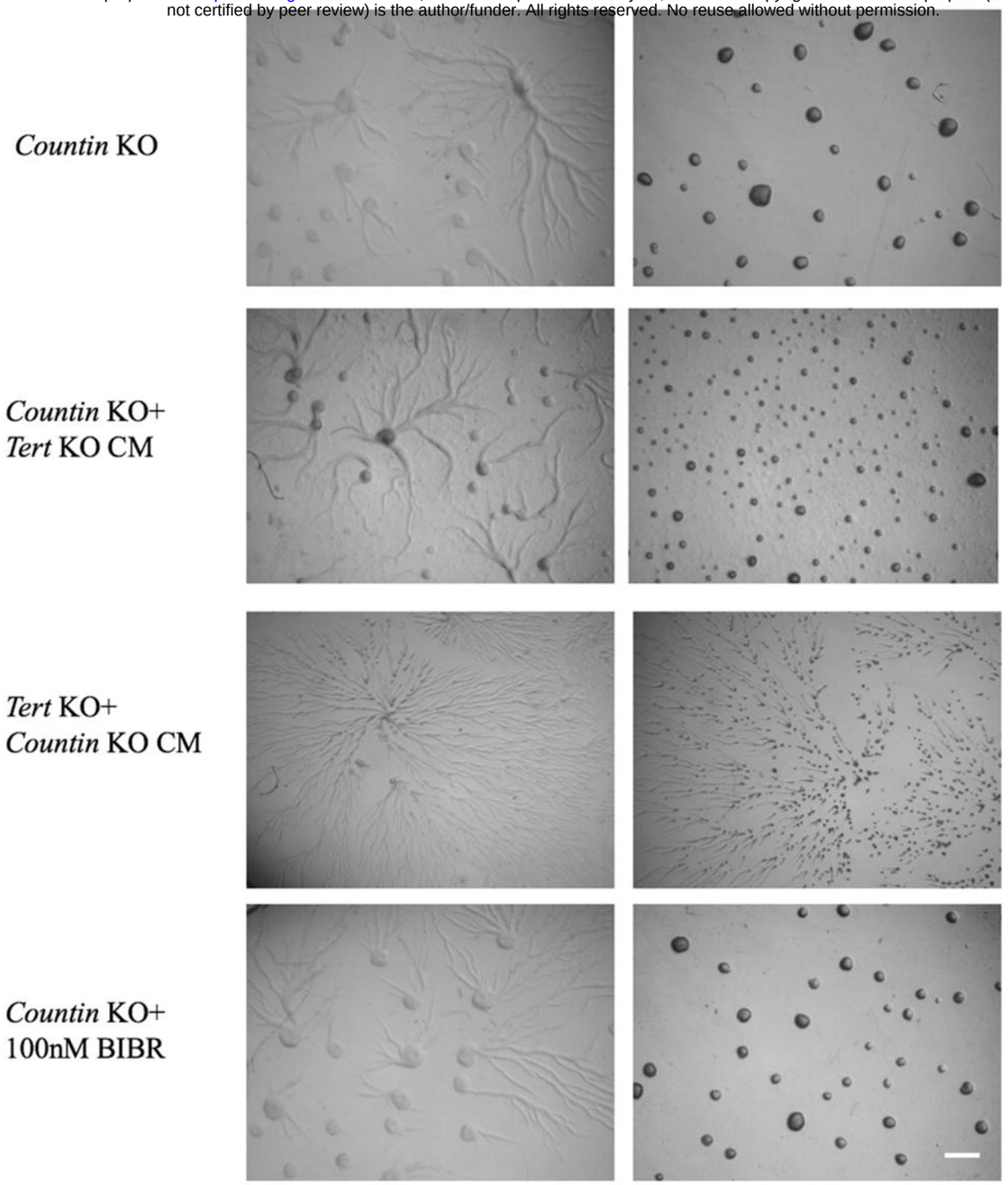

B

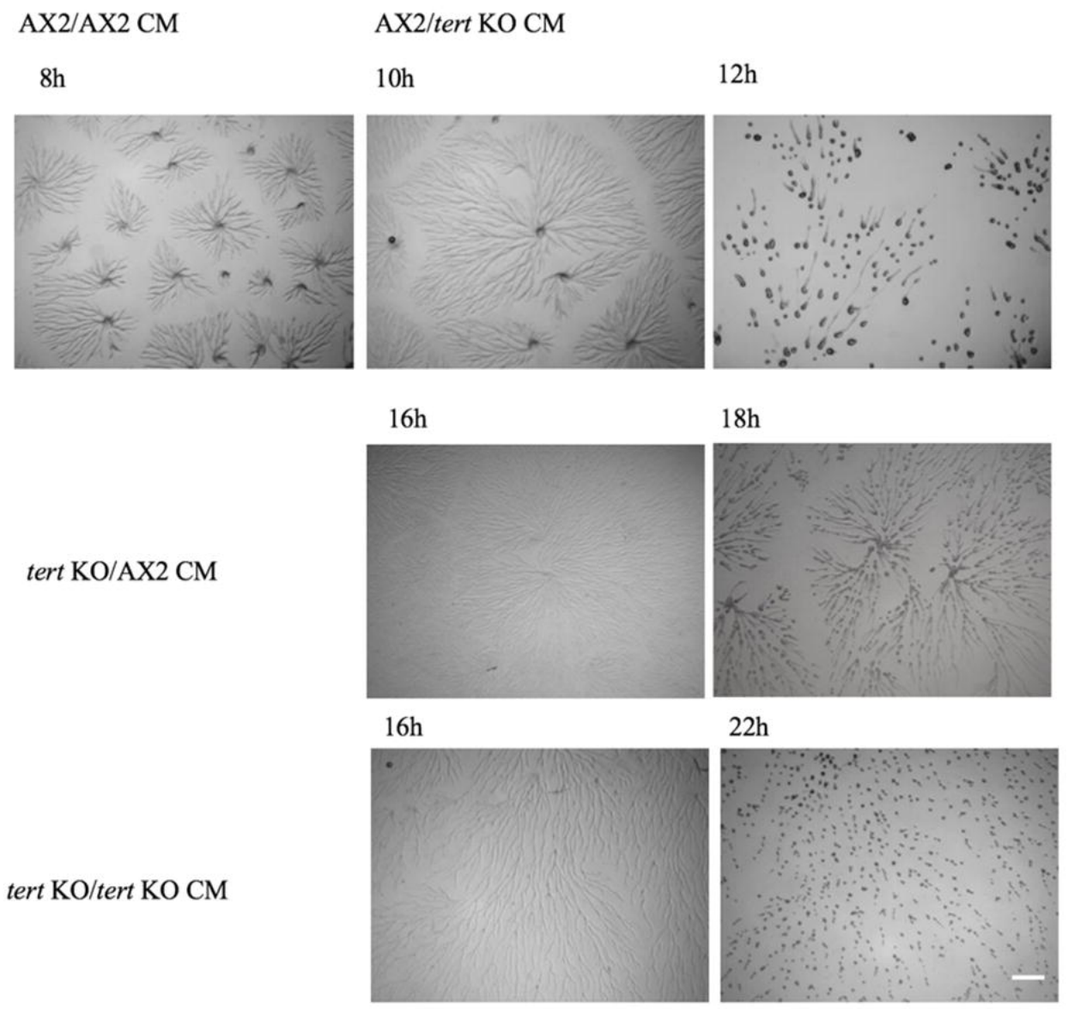

C

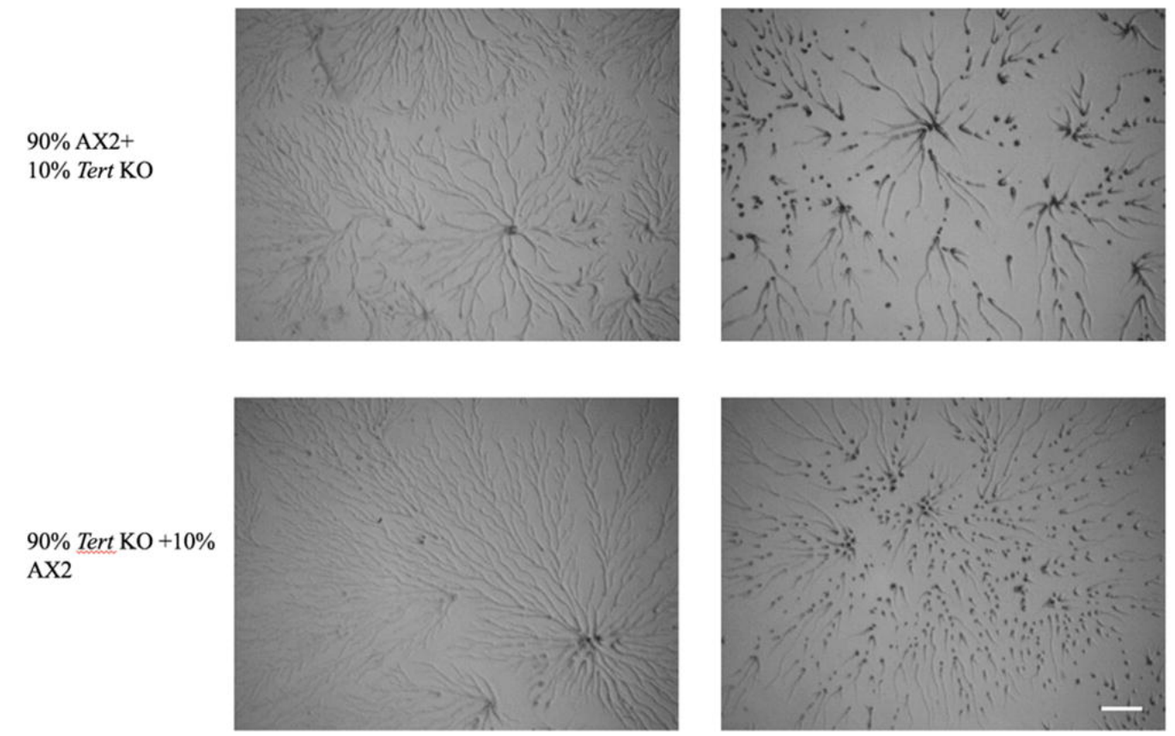

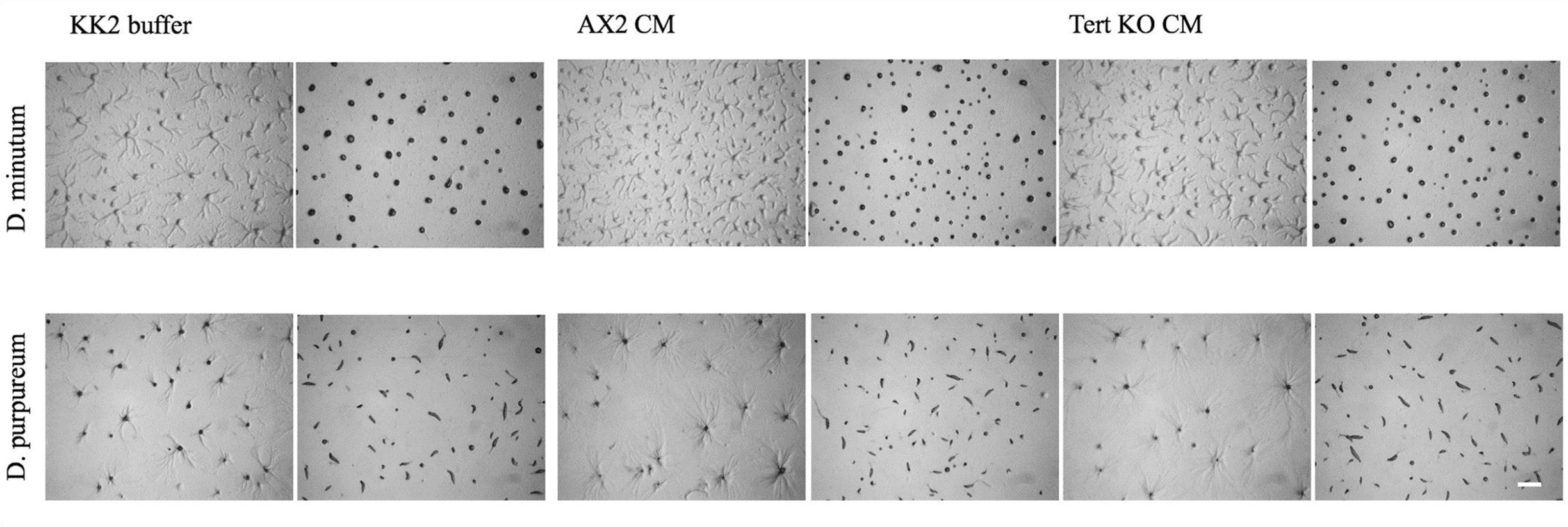
KK2 buffer
AX2 CM
Tert KO CM
D. minutum
D. purpureum

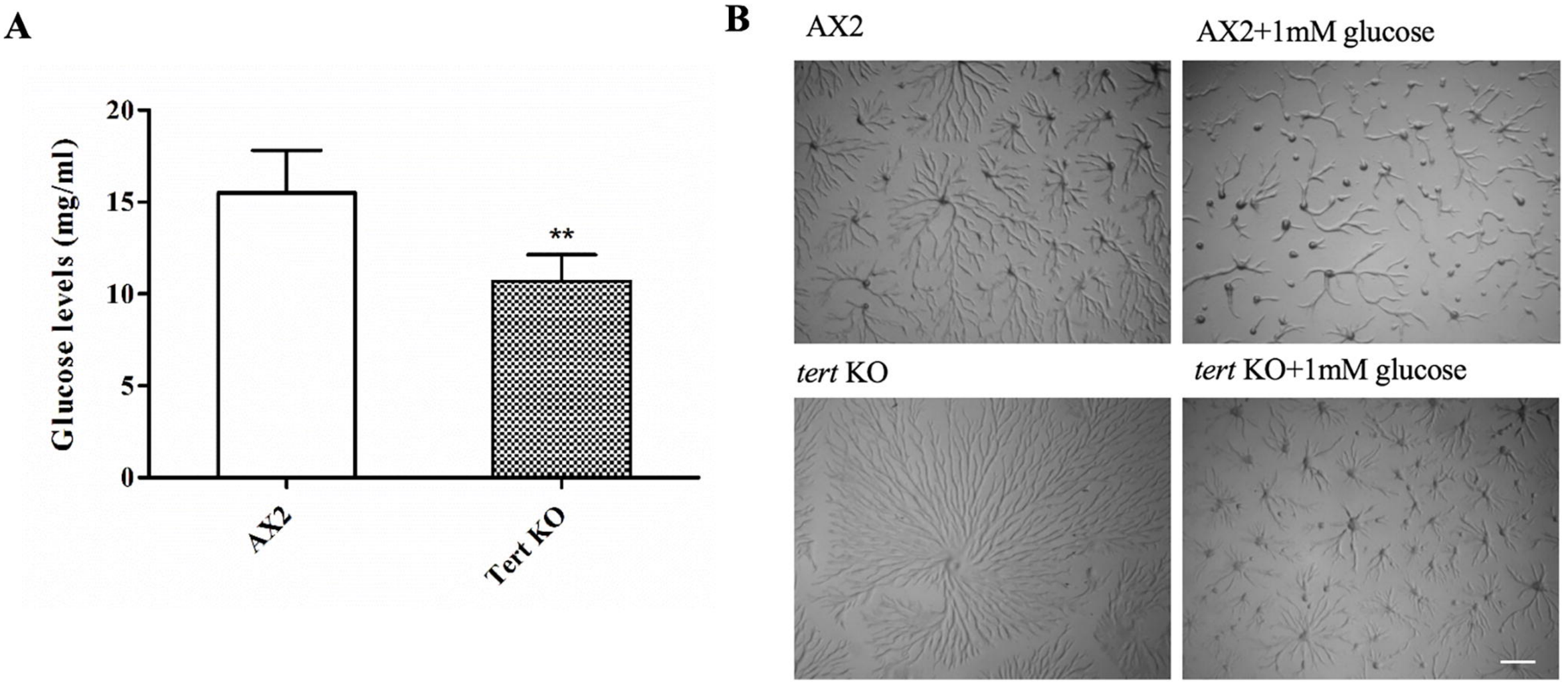
A
Glucose levels (mg/ml)
20
15
10
5
0
**
AX2
Tert KO
B
AX2
AX2+1mM glucose
tert KO
tert KO+1mM glucose

tert KO+
anti- AprA

tert KO+
anti- CfaD

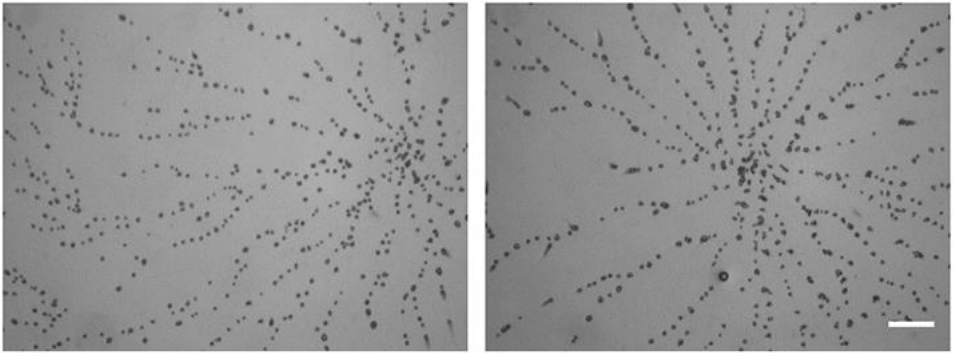

AX2

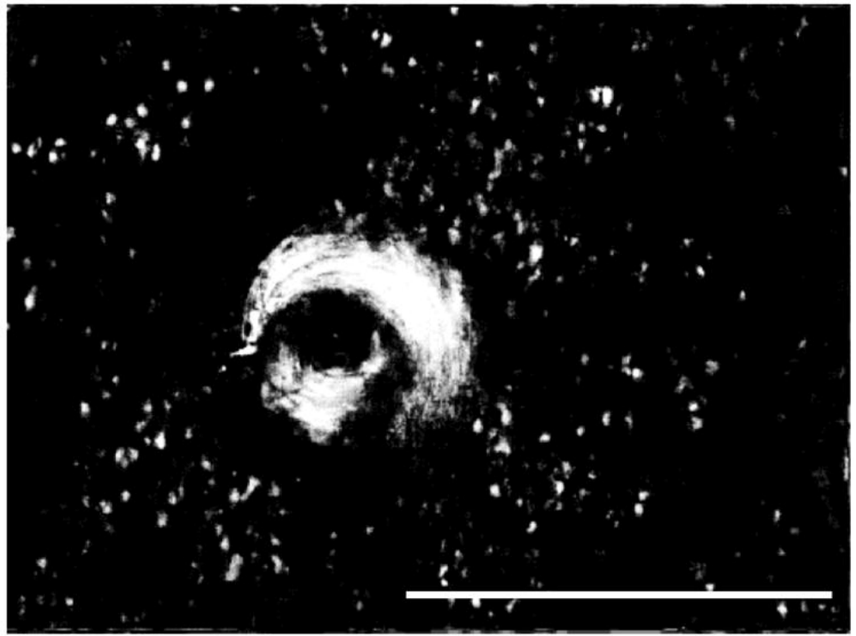

tert KO

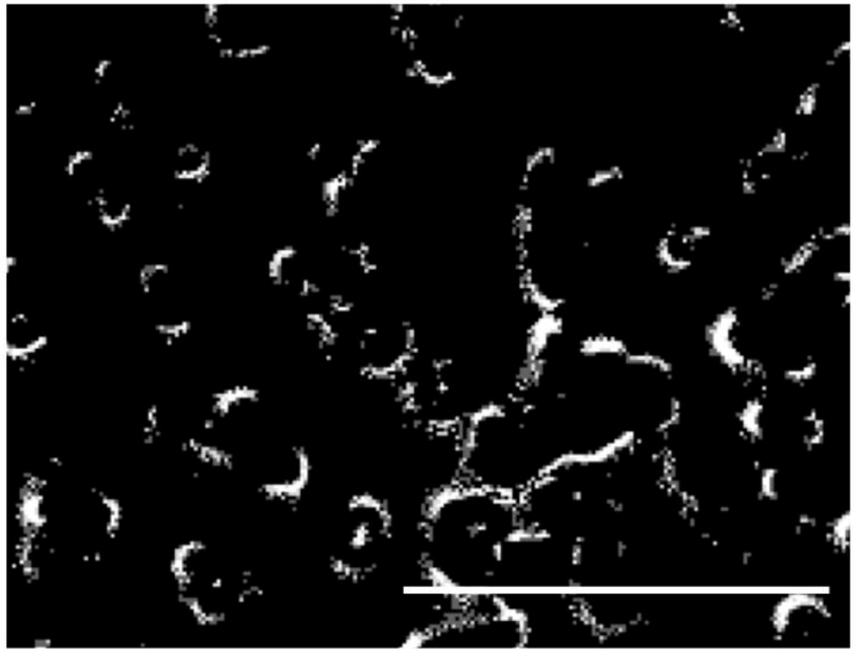

Rescue

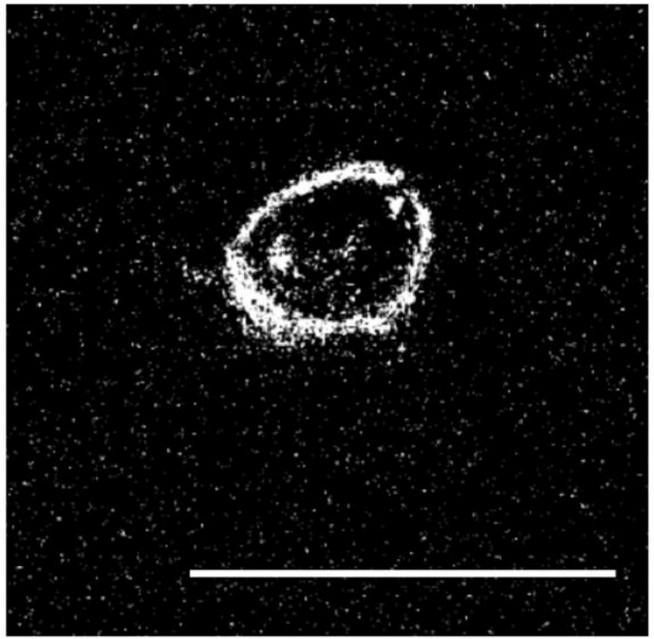

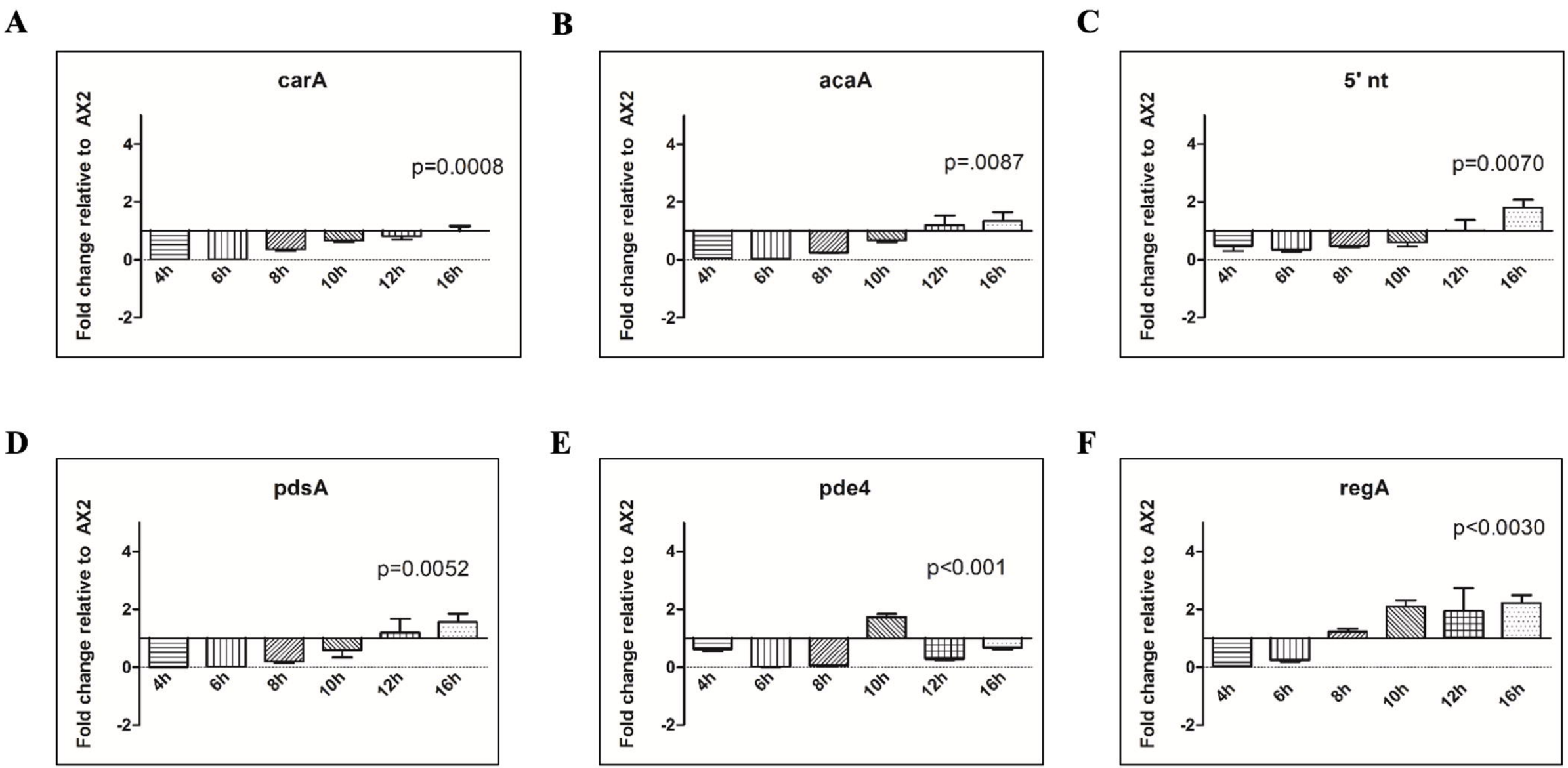
A
carA
p=0.0008
B
acaA
p=.0087
C
5' nt
p=0.0070
D
pdsA
p=0.0052
E
pde4
p<0.001
F
regA
p<0.0030
Fold change relative to AX2
4
2
0
-2
4h
6h
8h
10h
12h
16h

A

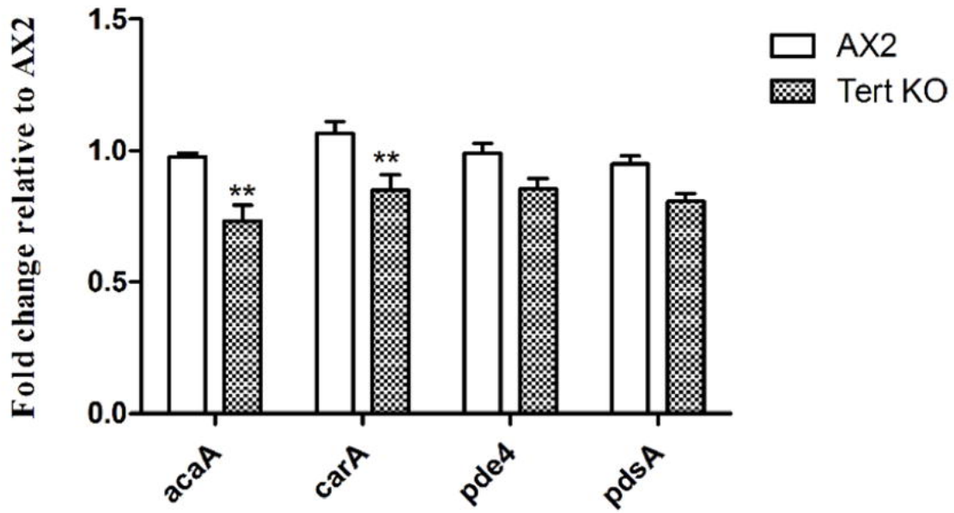
Fold change relative to AX2
1.5
1.0
0.5
0.0
**
**
acaA
carA
pde4
pdsA
AX2
Tert KO
During aggregation

B

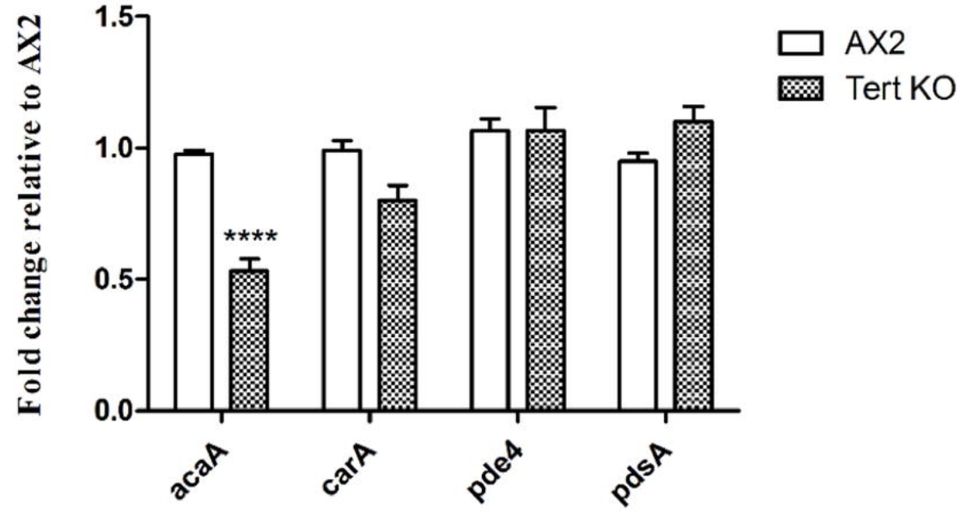
Fold change relative to AX2
1.5
1.0
0.5
0.0
****
acaA
carA
pde4
pdsA
AX2
Tert KO
During stream breaking

C

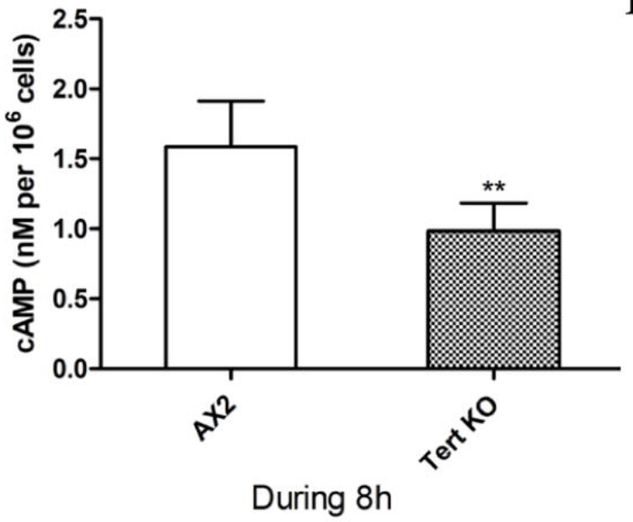
cAMP (nM per 10^6 cells)
2.5
2.0
1.5
1.0
0.5
0.0
**
AX2
Tert KO
During 8h

D

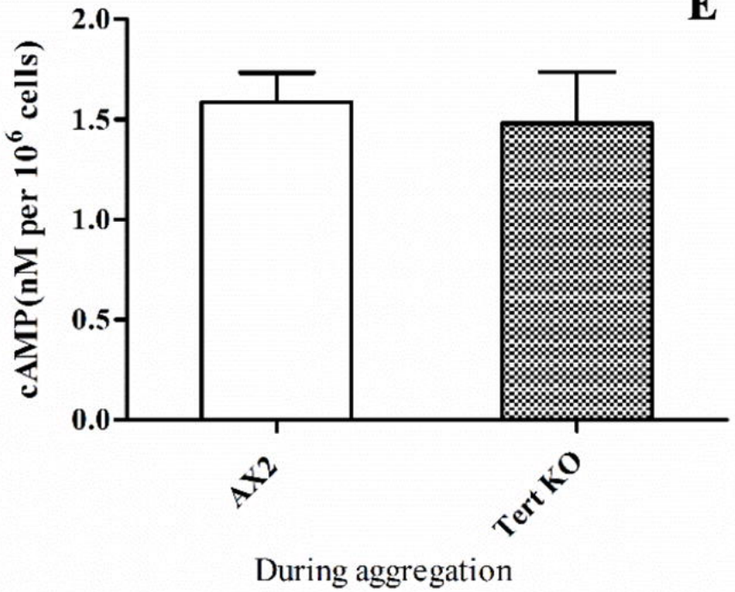
cAMP(nM per 10^6 cells)
2.0
1.5
1.0
0.5
0.0
AX2
Tert KO
During aggregation

E

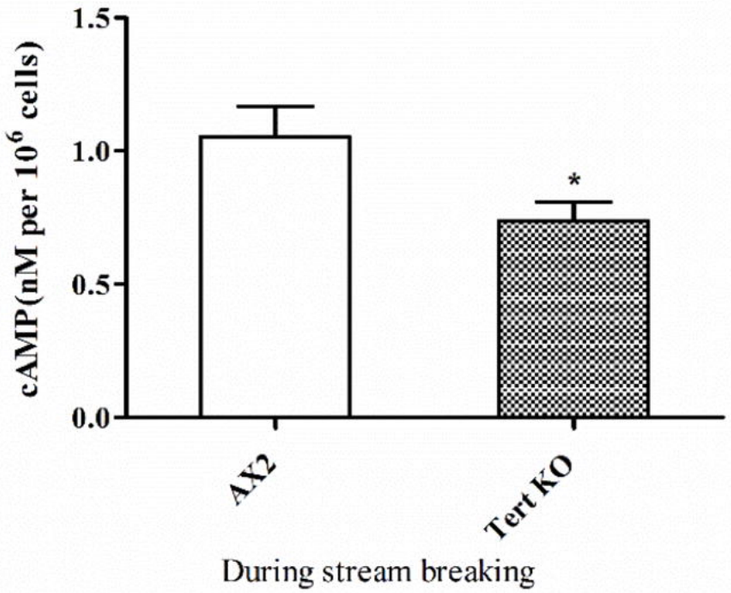
cAMP(nM per 10^6 cells)
1.5
1.0
0.5
0.0
*
AX2
Tert KO
During stream breaking

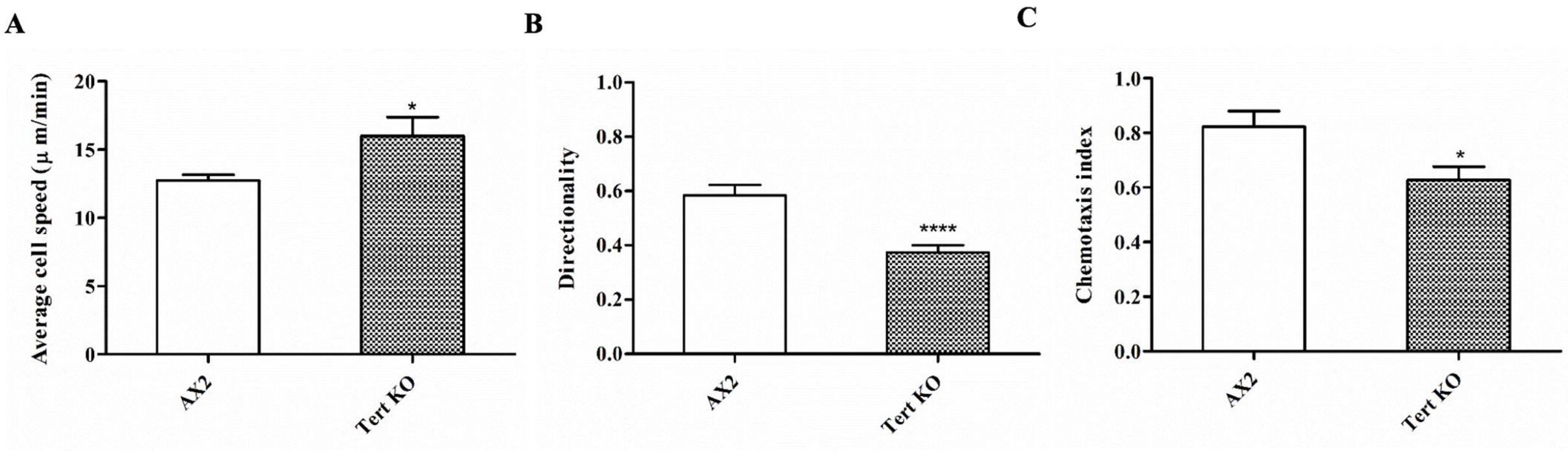
A
Average cell speed (μ m/min)
20
15
10
5
0
*
AX2
Tert KO
B
Directionality
1.0
0.8
0.6
0.4
0.2
0.0
****
AX2
Tert KO
C
Chemotaxis index
1.0
0.8
0.6
0.4
0.2
0.0
*
AX2
Tert KO

A

1h 4h 8h 20h 24h

AX2

tert KO

B

8h 10h 16h 30h 36h

AX2+
8Br cAMP

tert KO+
8Br cAMP

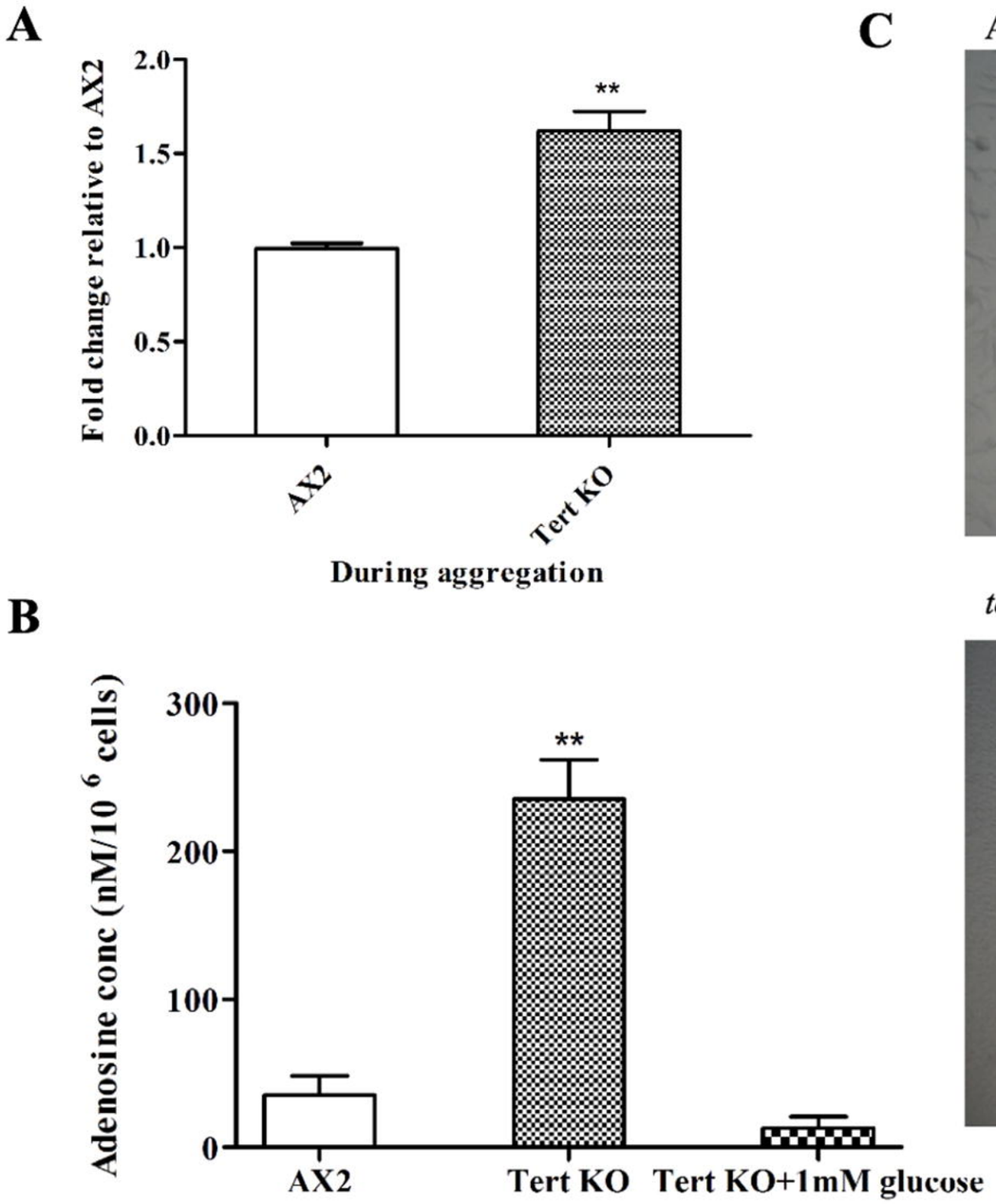
A
Fold change relative to AX2
2.0
1.5
1.0
0.5
0.0
**
AX2
Tert KO
During aggregation
B
Adenosine conc (nM/10 6 cells)
300
200
100
0
**
AX2
Tert KO
Tert KO+1mM glucose
C
AX2
AX2+1mM caffeine
tert KO
tert KO+1mM caffeine

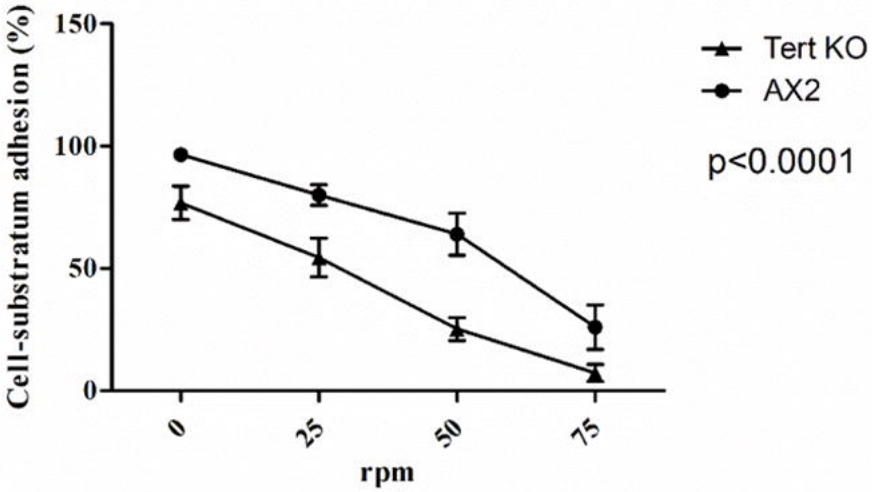
Cell-substratum adhesion (%)
150
100
50
0
0
25
50
75
rpm
Tert KO
AX2
p<0.0001

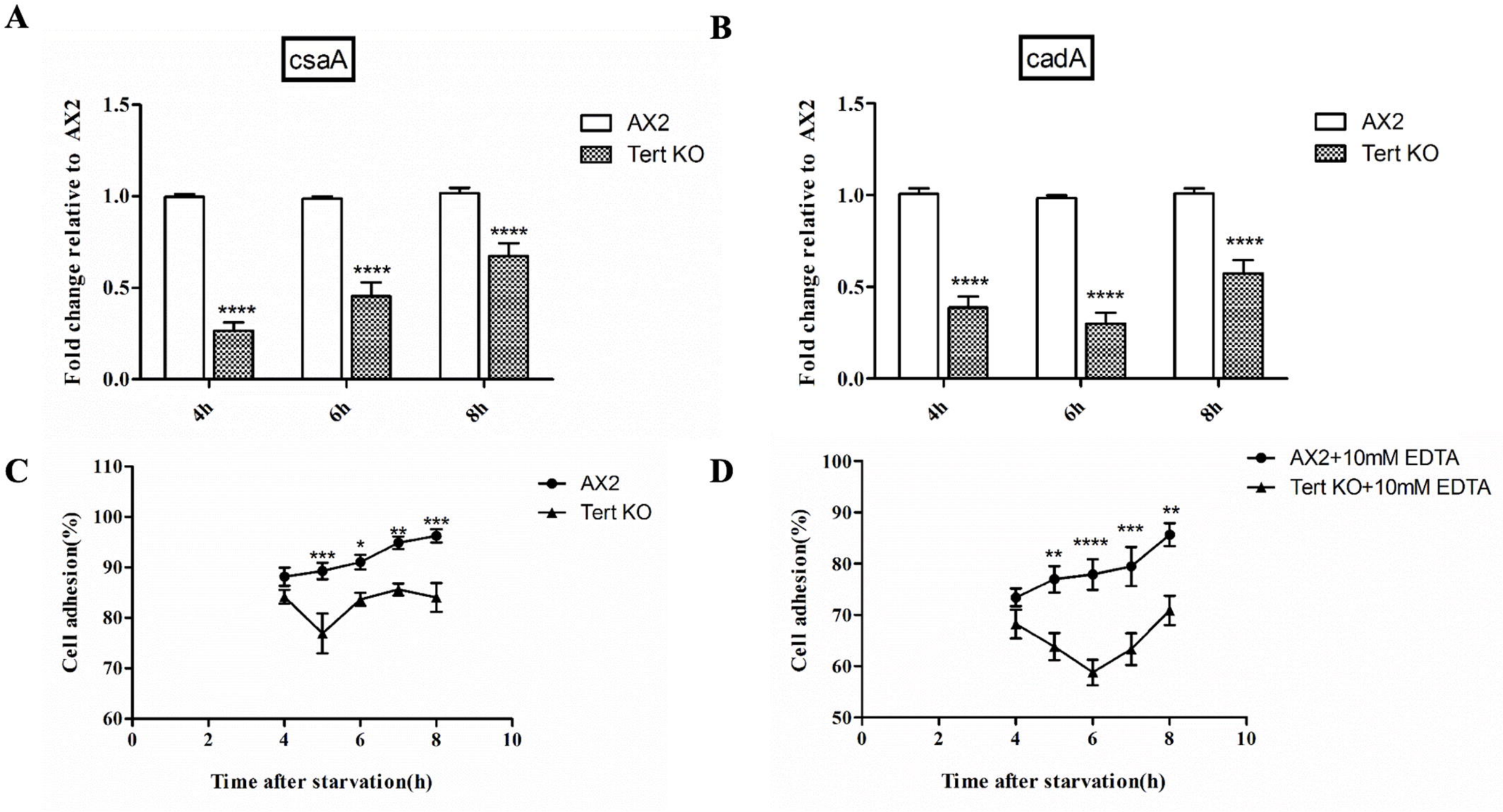
A
csaA
Fold change relative to AX2
1.5
1.0
0.5
0.0
AX2
Tert KO
****
****
****
4h
6h
8h
B
cadA
Fold change relative to AX2
1.5
1.0
0.5
0.0
AX2
Tert KO
****
****
****
4h
6h
8h
C
Cell adhesion(%)
110
100
90
80
70
60
AX2
Tert KO
***
*
**
***
0
2
4
6
8
10
Time after starvation(h)
D
Cell adhesion(%)
100
90
80
70
60
50
AX2+10mM EDTA
Tert KO+10mM EDTA
**
****
***
**
0
2
4
6
8
10
Time after starvation(h)

16h

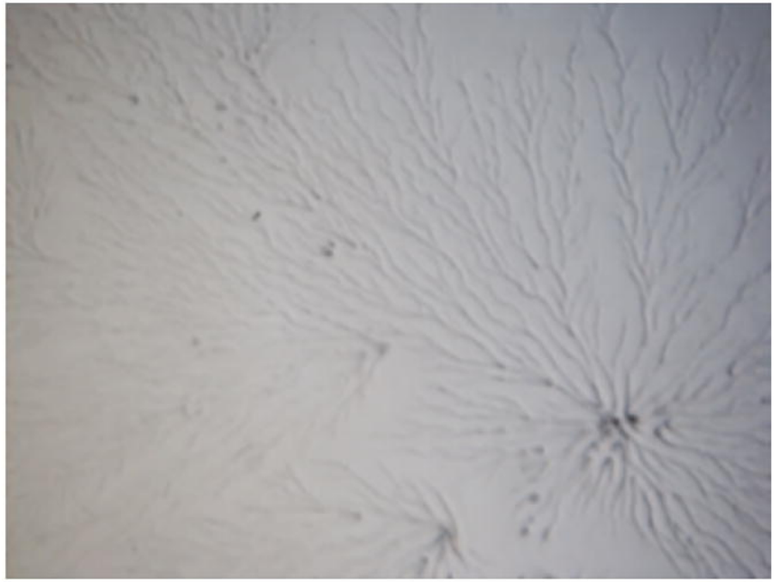

90% *tert* KO+
10% AX2

14h

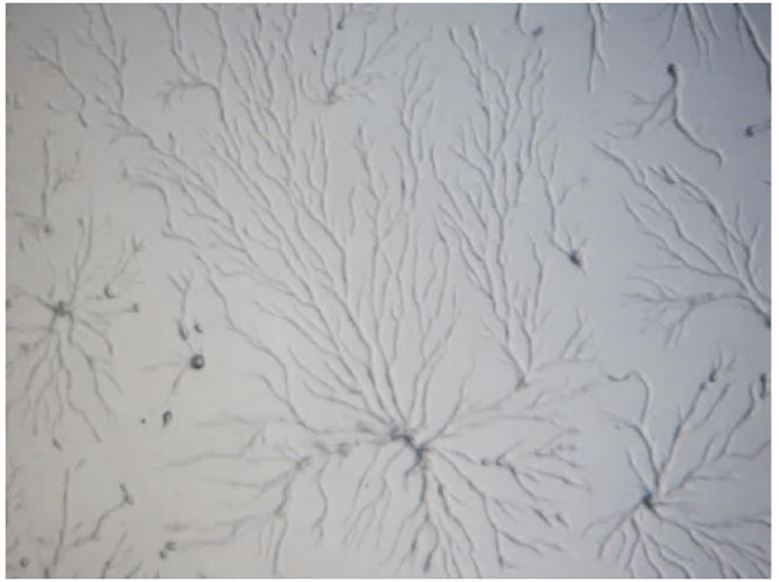

80% *tert* KO+
20% AX2

8h

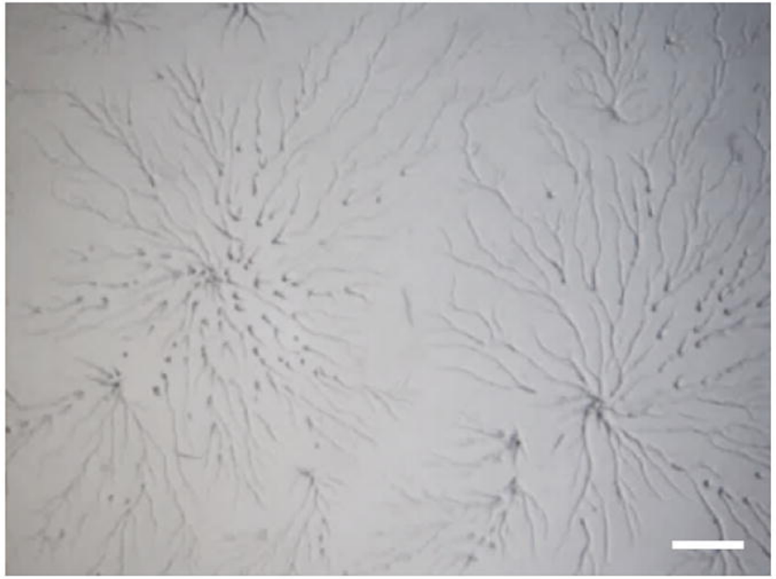

50% *tert* KO+
50% AX2

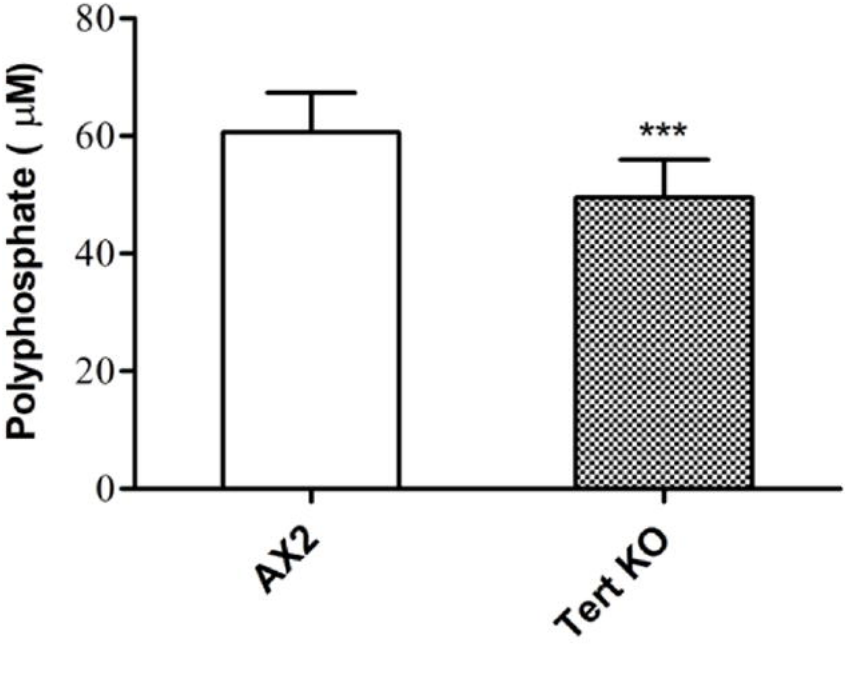
Polyphosphate (μM)
80
60
40
20
0
***
AX2
Tert KO

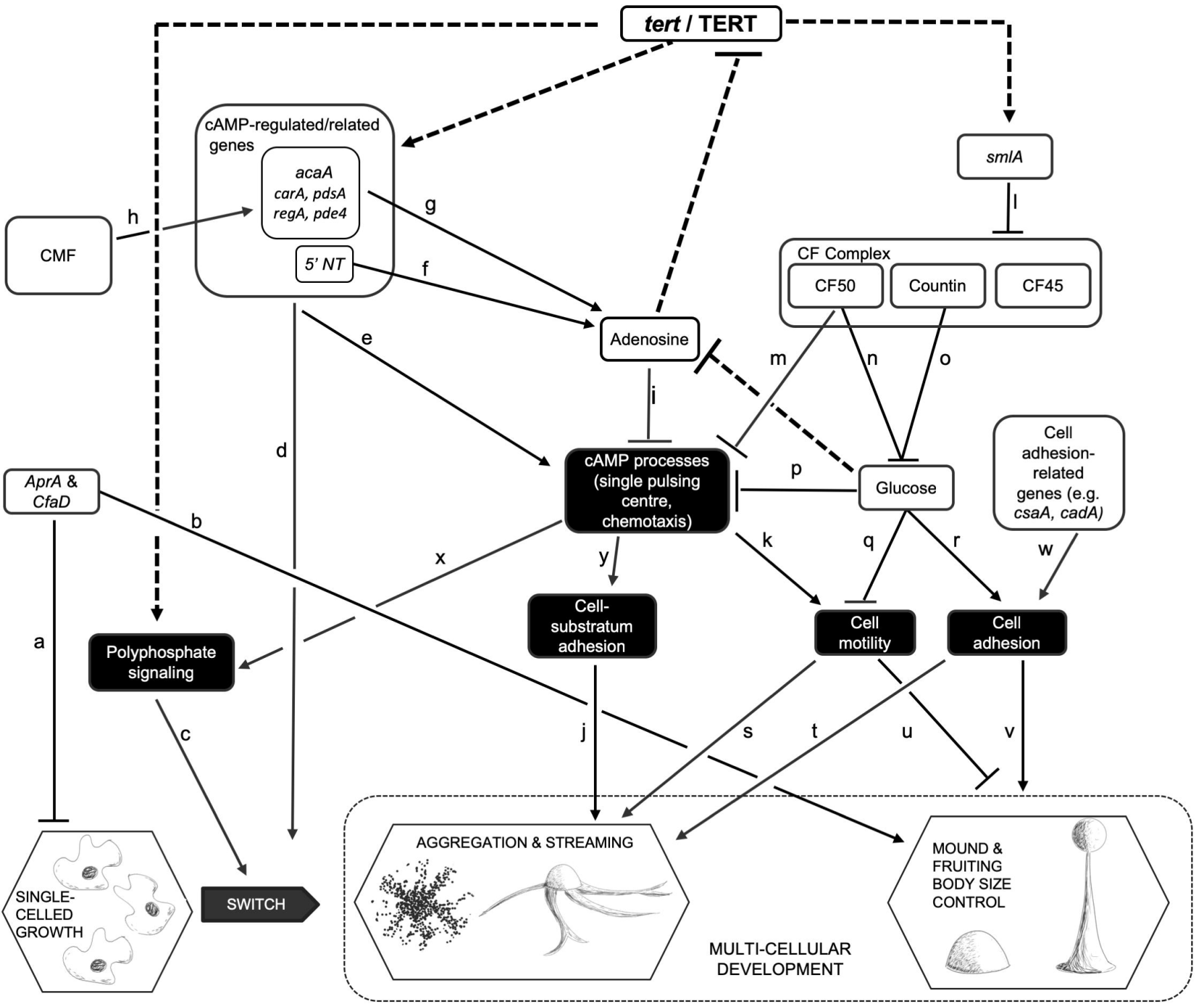
tert / TERT
cAMP-regulated/related genes
acaA
carA, pdsA
regA, pde4
5' NT
smlA
CMF
CF Complex
CF50
Countin
CF45
Adenosine
AprA & CfaD
cAMP processes (single pulsing centre, chemotaxis)
Glucose
Cell adhesion-related genes (e.g. csaA, cadA)
Cell-substratum adhesion
Cell motility
Cell adhesion
Polyphosphate signaling
SINGLE-CELLED GROWTH
SWITCH
AGGREGATION & STREAMING
MOUND & FRUITING BODY SIZE CONTROL
MULTI-CELLULAR DEVELOPMENT
a
b
c
d
e
f
g
h
i
j
k
l
m
n
o
p
q
r
s
t
u
v
w
x
y